

## SUPPLEMENTARY MATERIAL

**Uncovering the cryptic gene cluster *ahb* for 3-amino-4-hydroxybenzoate derived ahbamycins, by searching SARP regulator encoding genes in the *Streptomyces argillaceus* genome**

**Suhui Ye,<sup>†‡</sup> Brian Molloy,<sup>†</sup> Ignacio Pérez-Victoria,<sup>#</sup> Ignacio Montero,<sup>†‡</sup> Alfredo F. Braña,<sup>†</sup> Carlos Olano,<sup>†‡</sup> Sonia Arca,<sup>†</sup>, Jesús Martín,<sup>#</sup> Fernando Reyes,<sup>#</sup> José A. Salas<sup>†‡</sup> and Carmen Méndez<sup>†‡</sup> \***

<sup>†</sup>Departamento de Biología Funcional e Instituto Universitario de Oncología del Principado de Asturias (I.U.O.P.A), Universidad de Oviedo, Oviedo, Spain

<sup>‡</sup>Instituto de Investigación Sanitaria de Asturias (ISPA), Oviedo, Spain

<sup>#</sup>Fundación MEDINA, Centro de Excelencia en Investigación de Medicamentos Innovadores en Andalucía, Armilla, Granada, Spain.

\* Correspondence: Carmen Méndez ([cmendezf@uniovi.es](mailto:cmendezf@uniovi.es))

**Table S1.** Secondary metabolite gene clusters identified in *S. argillaceus* using antiSMASH 6.0

Cluster	Type	From	to	Predicted product
1	Butyrolactone	128,191	136,902	Unknown
2	Thiopeptide, PKS-like	171,777	225,841	Lactazole
3	Lanthipeptide-class III	401,954	424,038	SapB
4	NRPS-like	560,900	599,983	Unknown
5	Type II PKS, oligosaccharide	819,530	891,026	Mithramycin [18]
6	Lasso peptide, RiPP-like	1,034,574	1,056,293	Citrulassin D
7	Type II PKS	1,062,634	1,135,149	Spore pigment
8	NAPAA	1,638,191	1,672,045	$\epsilon$ -Poly-L-Lysine
9	Ectoine	1,875,607	1,886,011	Ectoine
10	TransAT-PKS-like, NRPS-like	2,346,931	2,423,228	Largimycins [20]
11	Melanin	2,866,180	2,875,776	Melanin
12	NI-Siderophore	2,971,449	2,982,026	Desferrioxamine B [19]
13	NRPS	3,407,302	3,461,180	Unknown
14	Terpene	5,232,759	5,251,815	Albaflavenone
15	Lanthipeptide-class II	5,316,978	5,340,023	Unknown
16	Siderophore	5,836,456	5,847,118	Unknown
17	Type I PKS	6,055,193	6,122,436	Argimycins P [17]
18	RiPP-like	6,309,087	6,319,089	Unknown
19	Terpene, butyrolactone	6,346,491	6,367,657	$\gamma$ -butyrolactone
20	NI-Siderophore	6,488,758	6,501,948	Unknown
21	Indole	6,700,660	6,721,835	Unknown
22	Terpene	6,916,343	6,942,645	Hopene
23	hgIE-KS-Type I PKS	6,991,030	7,043,896	Unknown
24	RiPP-like	7,270,946	7,281,161	Unknown
25	Melanin	7,430,918	7,441,352	Unknown
26	Terpene	7,564,422	7,590,728	Isorenieratene [19]
27	NRPS, Type I PKS	7,905,486	7,954,919	Antimycin [19]
28	Thioamide-NRP, NRPS, lanthipeptide-class II	8,021,022	8,112,102	Unknown
29	Lanipeptide-class I	8,224,262	8,249,451	Unknown
30	Lasso peptide	8,450,703	8,473,371	Unknown
31	NRPS	8,614,230	8,667,317	Unknown

hgIE-KS, Heterocyst glycolipid synthase-like PKS; NI-siderophore, NRPS-independent; NAPAA, Non-alpha poly-amino acids like  $\epsilon$ -Polylysine; NRPS, Non-Ribosomal Peptide Synthetase; PKS, Polyketide Synthase; RiPP, Ribosomally synthesized and post-translationally modified peptide.

**Table S2.** Predicted functions of genes in the *Streptomyces argillaceus* *ahb* gene cluster

<i>ahb</i> *	aa	Predicted function	<i>rah</i> *	<i>oah</i> *	<i>dah</i> *	<i>pah</i> *	<i>tah</i> *
<i>ahbO1</i>	281	2OG-Fe(II) oxygenase	WP_217236194 (94)	WP_189953973 (92)	WP_202919556 (92)	WP_079170665 (91)	WP_159539127 (89)
<i>ahbM1</i>	182	Methylated-DNA-[protein]-cysteine S-methyltransferase	WP_217236059 (89)	WP_189953954 (84)	WP_152883716 (89)	WP_055572750 (87)	WP_159536550 (88)
<i>ahbM2</i>	254	MGMT family protein	WP_217236195 (89)	WP_189953956 (89)	WP_152883945 (91)	WP_095534003 (86)	WP_159536551 (84)
<i>ahbR1</i>	197	RNA polymerase sigma factor	WP_217236060 (94)	WP_189953958 (93)	WP_152883713 (95)	WP_055572748 (93)	WP_159536552 (88)
<i>ahbR2</i>	258	AfsR/SARP family transcriptional regulator	WP_217236061 (91)	WP_189953960 (87)	WP_152883711 (93)	WP_055572747 (89)	WP_159536553 (87)
<i>ahbP1</i>	322	PfkB family carbohydrate kinase	WP_217236062 (90)	---	WP_152883709 (90)	---	WP_159536554 (89)
<i>ahbA</i>	406	Methionine adenosyltransferase	WP_217236063 (93)	WP_189948684 (93)	WP_152883707 (95)	WP_055572746 (92)	WP_159536555 (92)
<i>ahbS</i>	469	3-carboxy-cis,cis-muconate cycloisomerase	WP_217236064 (92)	WP_189948686 (89)	---	WP_055572745 (92)	WP_159536556 (86)
<i>ahbK1</i>	656	FAD/NAD(P)-binding protein	WP_217236065 (89)	WP_189948687 (89)	WP_152883705 (89)	WP_055572744 (86)	WP_159536557 (87)
<i>ahbM3</i>	337	Methyltransferase	WP_217236066 (94)	WP_189948689 (94)	WP_152883703 (94)	WP_055572743 (92)	WP_159536558 (94)
<i>ahbL1</i>	572	Acyl-CoA ligase	WP_217236067 (91)	WP_189948692 (92)	WP_152883700 (94)	WP_055572742 (91)	WP_159536559 (89)
<i>ahbO2</i>	584	FAD-dependent monooxygenase	WP_217236068 (90)	WP_189948694 (91)	WP_152883698 (92)	WP_055572741 (92)	WP_006124753 (ND)
<i>ahbR3</i>	290	AfsR/SARP family transcriptional regulator	WP_217236069 (93)	WP_229851348 (88)	WP_152883695 (90)	WP_074993823 (90)	WP_159536560 (80)
<i>ahbT1</i>	536	MFS transporter	WP_217236070 (86)	WP_189948698 (87)	WP_152892632 (91)	SDC40704.1 (89)	WP_159536561 (78)
<i>ahbK2</i>	268	SDR family oxidoreductase	WP_217236071 (99)	WP_189948700 (97)	WP_152892631 (98)	WP_055574900 (97)	WP_159536562 (99)
<i>ahbC</i>	208	Cupin domain-containing protein	WP_217236072 (97)	WP_229851349 (96)	WP_152892630 (98)	WP_074993828 (96)	WP_159536563 (96)
<i>ahbK3</i>	566	FAD-binding oxidoreductase	WP_217236073 (89)	WP_229851350 (90)	WP_152892629 (89)	WP_079039606 (90)	WP_159536564 (86)
<i>ahbM4</i>	220	Class I SAM-dependent methyltransferase	WP_217236074 (95)	WP_189948706 (95)	WP_152892628 (96)	WP_055570494 (95)	WP_159536565 (96)
<i>ahbK4</i>	188	Flavin reductase family protein	WP_217236075 (93)	WP_010070850 (ND)	WP_152892627 (92)	WP_055570493 (93)	WP_159536566 (89)
<i>ahbO3</i>	550	Aromatic ring hydroxylase	WP_217236076 (98)	WP_189948710 (98)	WP_152892626 (97)	WP_055570492 (99)	WP_159536567 (97)
<i>ahbT2</i>	405	MFS transporter	WP_217236077 (93)	WP_189948712 (91)	WP_152892625 (93)	WP_074993830 (93)	WP_159536568 (90)
<i>ahbR4</i>	305	Helix-turn-helix domain-containing protein	WP_217236078 (91)	WP_189948715 (87)	WP_152892624 (93)	WP_074993831 (88)	WP_159536569 (84)
<i>ahbL2</i>	584	Acyl-CoA ligase	WP_217236079 (86)	WP_189948717 (84)	WP_152892623 (90)	WP_055574594 (87)	WP_006124740 (ND)
<i>ahbH</i>	369	3-dehydroquinate synthase II family protein	WP_217236080 (97)	WP_189948720 (95)	WP_006124740 (ND)	WP_074993834 (97)	WP_159536570 (94)
<i>ahbI</i>	271	Fructose-bisphosphate aldolase	WP_217236196 (94)	WP_189948963 (97)	WP_152892636 (94)	WP_079039969 (95)	WP_159539129 (94)
<i>ahbK5</i>	550	FAD-binding oxidoreductase	WP_217236081 (92)	WP_229851351 (90)	WP_152892622 (93)	WP_095534094 (94)	WP_208026539 (90)
<i>ahbO4</i>	502	FAD-dependent monooxygenase	WP_217236082 (93)	WP_189948723 (90)	WP_152892621 (92)	WP_055694972 (94)	WP_159536571 (92)
<i>ahbF</i>	299	Methylenetetrahydrofolate reductase	WP_217236083 (91)	WP_189948725 (90)	WP_152892620 (89)	WP_055572786 (90)	WP_159536572 (89)
<i>ahbP2</i>	327	Carbohydrate kinase family protein	WP_217236084 (90)	WP_189948727 (89)	WP_152892635 (91)	WP_055572784 (91)	WP_159536574 (89)
<i>ahbR5</i>	100	Metal-binding protein	WP_217236197 (85)	WP_189948729 (80)	WP_202919764 (82)	WP_079039791 (86)	---
<i>ahbT3</i>	173	ABC transporter substrate-binding protein	WP_217236085 (87)	WP_229851352 (82)	WP_152892619 (84)	WP_055572783 (87)	---

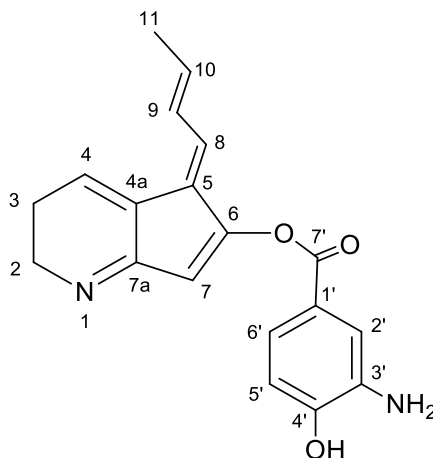
\* *ahb*, *S. argillaceus* ATCC 12956; *rah*, *Streptomyces* sp. AC555\_RSS877; *oah*, *S. roseolus* JCM 4411; *dah*, *S. adustus* NBRC 109810; *pah*, *S. prasinopilosus* CGMCC 4.3504; *tah*, *Streptomyces* sp. Tü 3180. Numbers between brackets indicate percentage of identical amino acids to the corresponded Ahb protein. ND, not determined. aa, number of amino acids of Ahb proteins.

**Table S3.** Oligonucleotides used for PCR amplification (restriction sites are underlined).

PRIMER	SEQUENCE 5'-3'
Delta ASU A fwd	GGGGAATTCGAAGAAGCGGACGTTCTCG
Delta ASU A rev	CGGCTGCAGATCGTGCAGGACGACTGG
Delta ASU B fwd	CGGGGATCCGGACACGGAGTGGTCCAG
Delta ASU B rev	TTGGATATCGGTACGTCAGGAGGAACACC
Delta 1705A fwd	CACGAATTCAGGTGAGGGGTGTGGTAAC
Delta 17054A rev	CGTTCCTGTACCGGGTCTC
Delta 1705B fwd	ACCGGATCCTGCAGCAGGTGAAGAAGAAG
Delta 1705B rev	GTTGATATCCGCGTAGTAGTCGGAGTTGG
AHBAermE fwd	GGATCCATCCGAACCCTGTGACCAG
AHBAermE rev	GAATTCTGACCACCACGTAGCAGAAC
SARP1304 fwd	CTGCAGGGCTCTCCTACGCTCTCTCA
SARP1304 rev	CTGCAGCTGCCTTGTCTCCATCAC
SARP1705 fwd	TCTAGATTCCAGAGGGATGACCTCCT
SARP1705 rev	TCTAGAGTGGGCGCCCTGGTCTGG
1705araC fwd	CATCACCTGGTGACCGGCGCGG
1705araC rev	CCCGGCTACCGGCTCGGGA
Check Delta AHBA fwd	ACCAGGACCGTTGTGTCATC
Check Delta AHBA rev	CTGTGACCAGGAACGAGGAG
d1705compr_A	AACATGTCGTCCCGGTC
d1705compr_B	TTCCAGAACAGCACCTTCT
ApraC rev	TCATTCTGTGGGCCGTAC
ApraC fw	TCATTCTGTGGGCCGTAC

**Table S4.** NMR data for **AHB18** (CD<sub>3</sub>OD, 24 °C, 500 MHz/125 MHz).

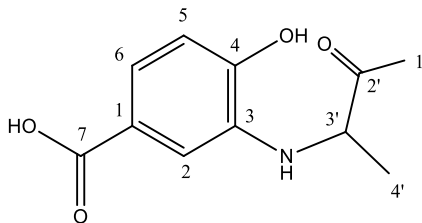
Position	$\delta_H$ (ppm), mult. ( <i>J</i> in Hz)	$\delta_C$ (ppm), type
2	3.57, at (7.6)	38.2, CH <sub>2</sub>
3	2.72, ddd (7.6, 7.6, 4.5)	22.9, CH <sub>2</sub>
4	7.09, at (4.5)	130.9, CH
4a	-	128.4, C
5	-	123.1, C
6	-	168.3, C
7	5.50, s	94.0, CH
7a	-	166.3, C
8	7.22, d (11.1)	129.1, CH
9	6.94, m	126.4, CH
10	6.46, m	142.9, CH
11	2.03, br d (6.8)	17.8, CH <sub>3</sub>
1'	-	126.4, C
2'	7.86, br s	127.8, CH
3'	-	124.3, C
4'	-	155.0, C
5'	7.00 d, (8.9)	115.7, CH
6'	7.87, br d	130.4, CH
7'	-	170.5, C
<b>Nitrogen</b>	<b><math>\delta_N</math> (ppm)</b>	
1	108	
3' NH <sub>2</sub>	110	



<sup>13</sup>C chemical shifts determined from the indirect dimension of HSQC and HMBC spectra. <sup>15</sup>N chemical shift scale corresponds to Bruker's default ammonia reference.

**Table S5a.** NMR data for keto form of **AHB74** (CD<sub>3</sub>OD, 24 °C, 500 MHz/125 MHz).

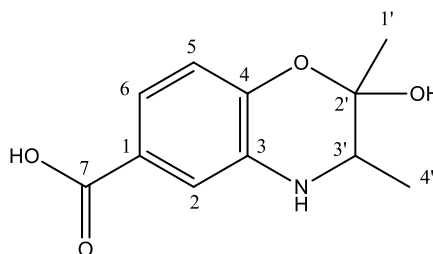
Position	$\delta_H$ (ppm), mult. ( <i>J</i> in Hz)	$\delta_C$ (ppm), type
1	-	122.3, C
2	6.96, d (1.9)	111.2, CH
3	-	135.5, C
4	-	149.2, C
5	6.76, d (8.1)	113.5, CH
6	7.18, dd (8.1, 1.9)	120.2, CH
7	-	168.1, C
1'	2.14, s	26.0, CH <sub>3</sub>
2'	-	210.5, C
3'	4.12, quart (7.0)	58.1, CH
4'	1.34, d (7.0)	17.4, CH <sub>3</sub>



<sup>13</sup>C chemical shifts determined from the indirect dimension of HSQC and HMBC spectra.

**Table S5b.** NMR data for hemiketal form of **AHB74** (CD<sub>3</sub>OD, 24 °C, 500 MHz/125 MHz). Non isochronous signals of both hemiketal epimers (at position 2') are indicated.

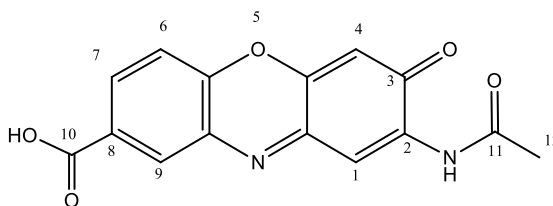
Position	$\delta_H$ (ppm), mult. ( <i>J</i> in Hz)	$\delta_C$ (ppm), type
1	-	123.5, C
2	7.23, m	115.9, CH
3	-	133.2, C
4	-	146.4, C
5	6.68, d (8.3)	116.3, CH
6	7.17, m	119.9, CH
7	-	167.9, C
1' (epimer a)	1.41, s	24.7, CH <sub>3</sub>
1' (epimer b)	1.25, s	21.3, CH <sub>3</sub>
2' (epimer a)	-	96.4, C
2' (epimer b)	-	98.5, C
3' (epimer a)	3.14, quart. (6.3)	52.5, CH
3' (epimer b)	3.13, quart. (6.3)	
4' (epimer a)	1.14, d (6.3)	16.3, CH <sub>3</sub>
4' (epimer b)	1.10, d (6.3)	16.7, CH <sub>3</sub>



<sup>13</sup>C chemical shifts determined from the indirect dimension of HSQC and HMBC spectra.

**Table S6.** NMR data for **AHB75** (DMSO-d<sub>6</sub>, 24 °C, 500 MHz/125 MHz).

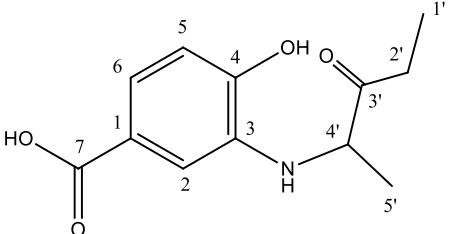
Position	$\delta_H$ (ppm), mult. ( <i>J</i> in Hz)	$\delta_C$ (ppm), type
1a	-	149.1, C
1	8.28, s	113.9, CH
2	-	138.5, C
2-NH	9.77, s	-
3	-	180.2, C
4	6.54, s	104.9, CH
4a	-	150.2, C
5a	-	146.3, C
6	7.63, d (8.6)	117.1, CH
7	8.12, dd (8.6, 2.0)	132.6, CH
8	-	128.6, C
9	8.29, d (2.0)	130.8, CH
9a	-	133.6, C
10	-	166.6, C
11	-	171.3, C
12	2.25, s	24.9, CH



<sup>13</sup>C chemical shifts determined from the indirect dimension of HSQC and HMBC spectra.

**Table S7a.** NMR data for the keto form of **AHB76** (DMSO-d<sub>6</sub>, 24 °C, 500 MHz/125 MHz).

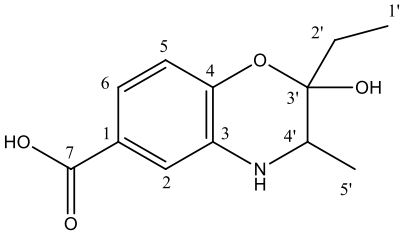
Position	$\delta_H$ (ppm), mult. ( <i>J</i> in Hz)	$\delta_C$ (ppm), type
1	-	122.5, C
2	6.92, d (1.6)	110.9, CH
3	-	135.9, C
4	-	149.0, C
5	6.74, d (8.1)	113.4, CH
6	7.15, dd (8.1, 1.8)	119.8, CH
7	-	168.3, C
1'	0.93, m	8.0, CH <sub>3</sub>
2'	2.61, m 2.50, m	31.1, CH <sub>2</sub>
3'	-	213.2, C
4'	4.14, quart (7.0)	57.4, CH
5'	1.33, d (7.0)	17.8, CH <sub>3</sub>



<sup>13</sup>C chemical shifts determined from the indirect dimension of HSQC and HMBC spectra.

**Table S7b.** NMR data for the hemiketal form of **AHB76** (DMSO-d<sub>6</sub>, 24 °C, 500 MHz/125 MHz). Non isochronous signals of both hemiketal epimers (at position 3') are indicated.

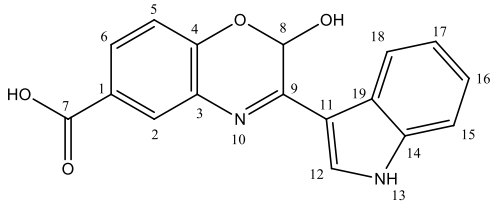
Position	$\delta_H$ (ppm), mult. ( <i>J</i> in Hz)	$\delta_C$ (ppm), type
1	-	123.7, C
2	7.20, d (1.2)	115.7, CH
3	-	134.0, C
4	-	146.2, C
5	6.67, d (8.1)	116.2, CH
6	7.12, m	119.4, CH
7	-	168.1, C
1' (epimer a)	0.96, t (7.5)	7.6, CH <sub>3</sub>
1' (epimer b)	0.90, t (7.6)	7.0, CH <sub>3</sub>
2' (epimer a)	1.77, dq (15.2, 7.5); 1.66, m	30.2, CH <sub>2</sub>
2' (epimer b)	1.60, m	26.9, CH <sub>2</sub>
3' (epimer a)	-	97.7, C
3' (epimer b)	-	98.8, C
4' (epimer a)	3.18, quart. (6.5)	50.1, CH
4' (epimer b)	3.22, m	51.5, CH
5' (epimer a)	1.10, d (6.5)	16.1, CH <sub>3</sub>
5' (epimer b)	1.06, d (6.5)	16.9, CH <sub>3</sub>



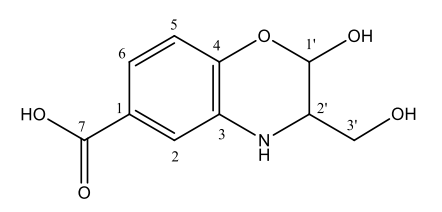
<sup>13</sup>C chemical shifts determined from the indirect dimension of HSQC and HMBC spectra.

**Table S8.** NMR data for **AHB77** (DMSO-d<sub>6</sub>, 24 °C, 500 MHz/125 MHz).

Position	$\delta_H$ (ppm), mult. ( <i>J</i> in Hz)	$\delta_C$ (ppm), type
1	-	125.2, C
2	7.99, d (2.1)	128.4, CH
3	-	134.0, C
4	-	148.2, C
5	7.10, d (8.3)	117.2, CH
6	7.73, m	128.4, CH
7	-	167.6, C
8	6.42, d (6.7)	85.7, CH
8-OH	7.74, m	-
9	-	156.8, C
11	-	112.5, C
12	8.16, d (2.9)	131.2, CH
13	11.88, br s	-
14	-	137.5, C
15	7.50, br dt (7.6)	112.5, CH
16	7.25, m	123.3, CH
17	7.22, m	121.6, CH
18	8.60, br dd (7.3)	123.1, CH
19	-	125.9, C


<sup>13</sup>C chemical shifts determined from the indirect dimension of HSQC and HMBC spectra.**Table S9.** NMR data for **AHB118** (DMSO-d<sub>6</sub>, 24 °C, 500 MHz/125 MHz). Non isochronous signals of both hemicetal epimers (at position 1') are indicated.

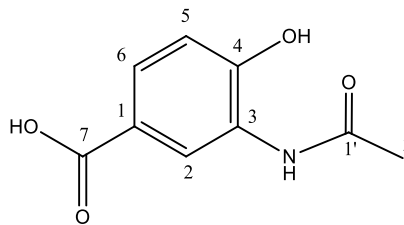
Position	$\delta_H$ (ppm), mult. ( <i>J</i> in Hz)	$\delta_C$ (ppm), type
1	-	123.7, C
2	7.23, d (1.8)	115.5, CH
3	-	134.0, C
4	-	145.2, C
5	6.70, d (8.2)	116.4, CH
6	7.12, dd (8.2, 1.8)	119.0, CH
7	-	168.0, C
1' (epimer a)	5.29, d (3.2)	90.4, CH
1' (epimer b)	5.44, d (1.4)	90.3, CH
2' (epimer a)	3.11, ddd (6.3, 6.3, 3.3)	55.7, CH
2' (epimer b)	3.27, ddd (6.4, 6.4, 1.9)	54.9, CH
3' (epimer a)	3.45, m; 3.35, m	62.0, CH <sub>2</sub>
3' (epimer b)	3.57, dd (6.3, 3.8); 3.43, m	61.1, CH <sub>2</sub>


<sup>13</sup>C chemical shifts determined from the indirect dimension of HSQC and HMBC spectra.



**Table S10.** NMR data for **AHB119** (DMSO-d<sub>6</sub>, 24 °C, 500 MHz/125 MHz).

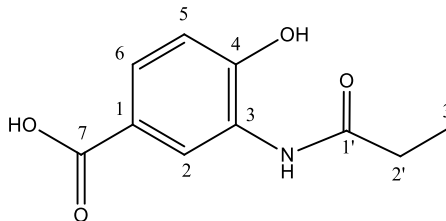
Position	$\delta_H$ (ppm), mult. ( <i>J</i> in Hz)	$\delta_C$ (ppm), type
1	-	121.8, C
2	8.42, d (1.9)	124.1, CH
3	-	126.6, C
3-NH	9.30, s	-
4	-	152.8, C
5	6.92, d (8.3)	115.5, CH
6	7.57, dd (8.3, 1.9)	126.8, CH
7	-	167.6, C
1'	-	169.5, C
2'	2.11, s	24.1, CH <sub>3</sub>



<sup>13</sup>C chemical shifts determined from the indirect dimension of HSQC and HMBC spectra.

**Table S11.** NMR data for **AHB120** (DMSO-d<sub>6</sub>, 24 °C, 500 MHz/125 MHz).

Position	$\delta_H$ (ppm), mult. ( <i>J</i> in Hz)	$\delta_C$ (ppm), type
1	-	121.8, C
2	8.42, d (1.9)	124.1, CH
3	-	126.6, C
3-NH	9.30, s	-
4	-	152.8, C
5	6.92, d (8.3)	115.5, CH
6	7.57, dd (8.3, 1.9)	126.8, CH
7	-	167.6, C
1'	-	173.1, C
2'	2.41, quart. (7.6)	29.7, CH <sub>2</sub>
3'	1.08, t (7.6)	10.2, CH <sub>3</sub>



<sup>13</sup>C chemical shifts determined from the indirect dimension of HSQC and HMBC spectra.

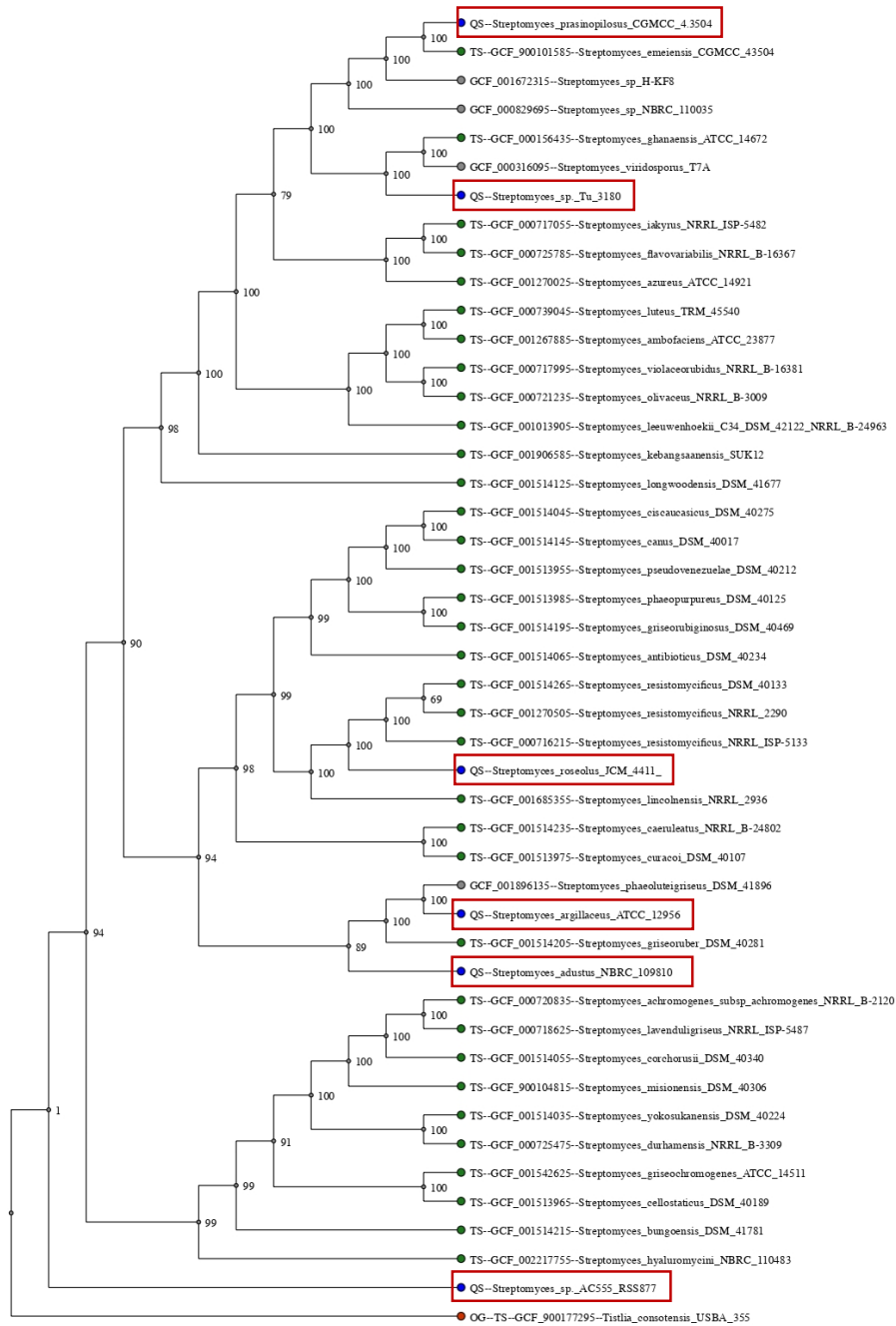


**Figure S1.** Phylogenetic analysis of *Streptomyces* strains containing *ahb* BGCs. The maximum-likelihood tree of the concatenated nucleotide sequences of 82 housekeeping genes were generated with autoMLST server [49]. An IQ-TREE Ultrafast Bootstrap analysis (1000 replicates) was performed, and ModelFinder was applied to find the optimal model for tree building. Genbank files containing the genomic sequences from the strains under study were used as inputs for phylogenetic inference using “de novo mode” pipeline, as in Cenicerós et al. [23]. Strains used for *ahb* clusters comparison are squared in red. TS: Type strain, QS: query sequence, OG: outgroup.

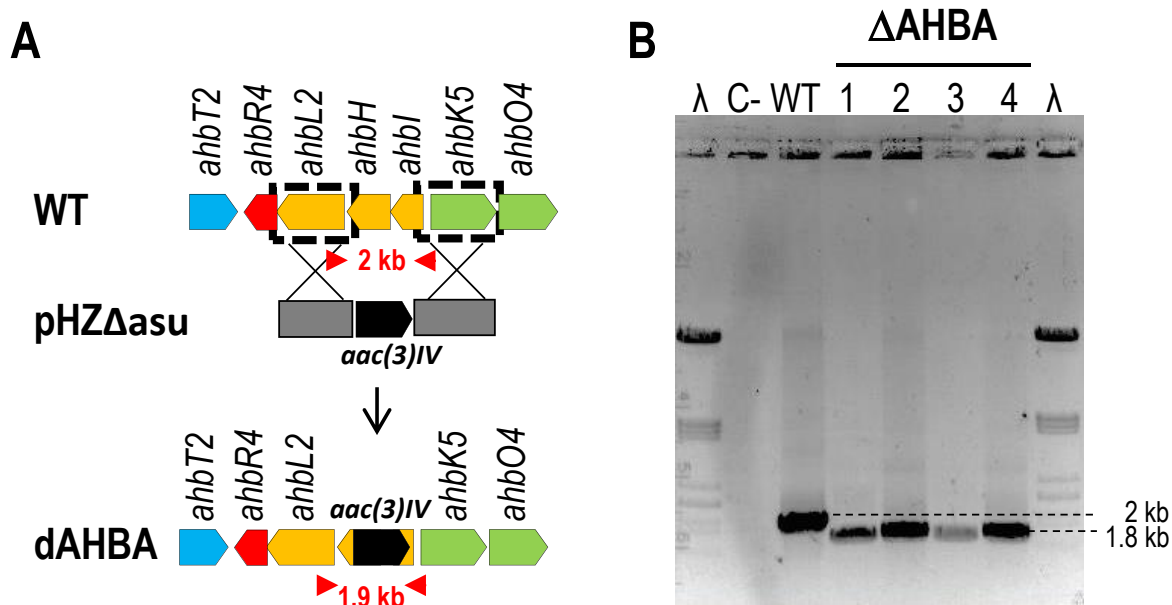


**Figure S2.** Generation of *S. argillaceus* ΔAHBA. (A) Graphical representation of the replacement event for the generation of ΔAHBA mutant strain; (B) PCR analysis of ΔAHBA mutant strain. PCR products from the wild type (WT) strain and from the ΔAHBA mutant using oligonucleotides Check Delta AHBA fw (a) and Check Delta AHBA rev (b). Negative control of the PCR reaction (-). λ, PstI-digested Lambda DNA. *aac(3)/IV*, apramycin resistance gene.

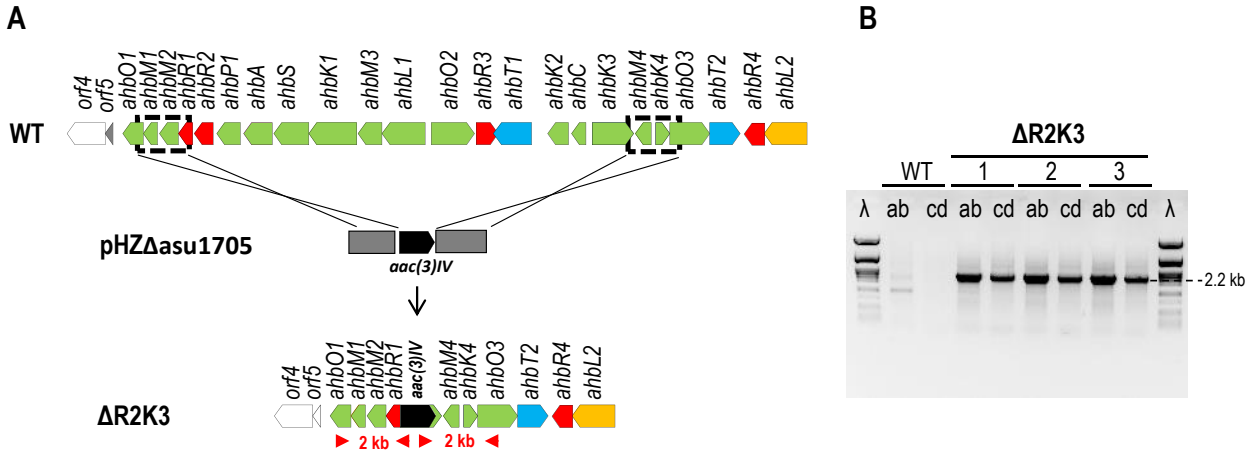


**Figure S3.** Generation of *S. argillaceus*  $\Delta R2K3$ . (A) Graphical representation of the replacement event for the generation of  $\Delta R2K3$  mutant strain; (B) PCR analysis of  $\Delta R2K3$  mutant strain. PCR products from the  $\Delta R2K3$  mutant using oligonucleotides d1705compr\_A (a) and ApraC rev (b), or d1705compr\_B (c) and ApraC fw (d). Oligonucleotides b and c anneals at the apramycin resistance gene. WT was used as negative control.  $\lambda$ , PstI-digested Lambda DNA. *aac(3)/IV*, apramycin resistance gene

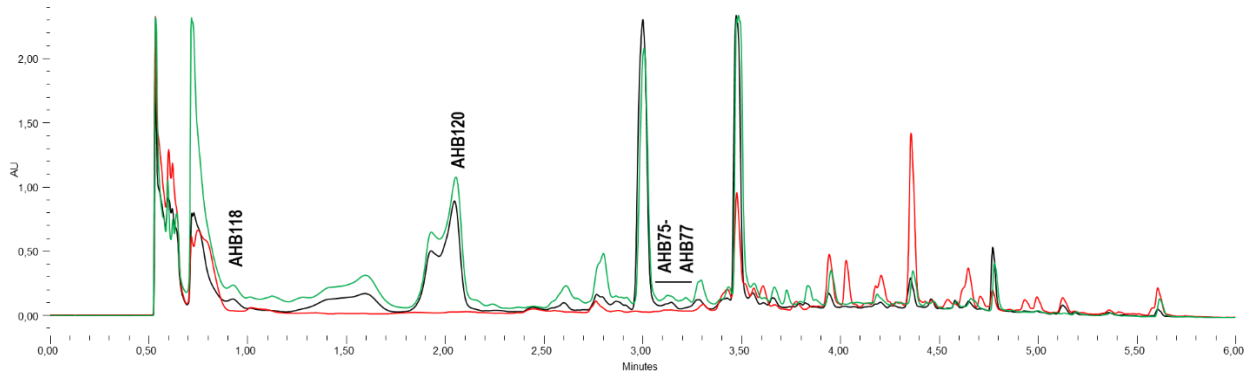


**Figure S4.** UPLC analysis of extracts of complemented *S. argillaceus*  $\Delta AHBA$  mutant. Chromatograms at 230 nm of extracts of *S. argillaceus* WT-pREG (black line), *S. argillaceus*  $\Delta AHBA$ -pREG (red line) and *S. argillaceus*  $\Delta AHBA$ -pREG-pSETeAHBAHyg (green line).

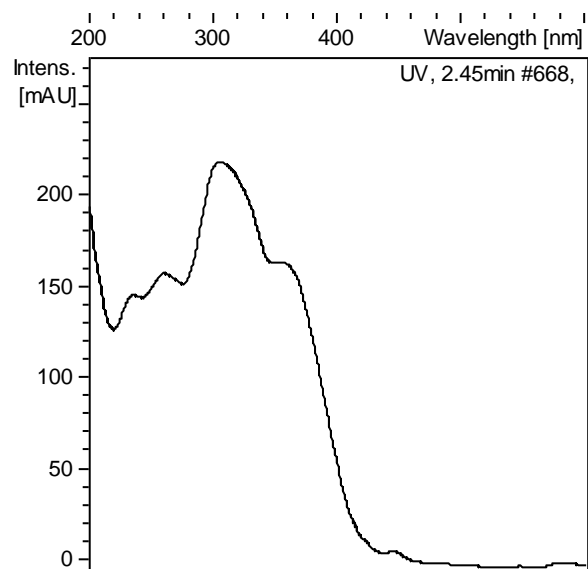


**Figure S5.** UV-vis (DAD) spectrum of **AHB18**.

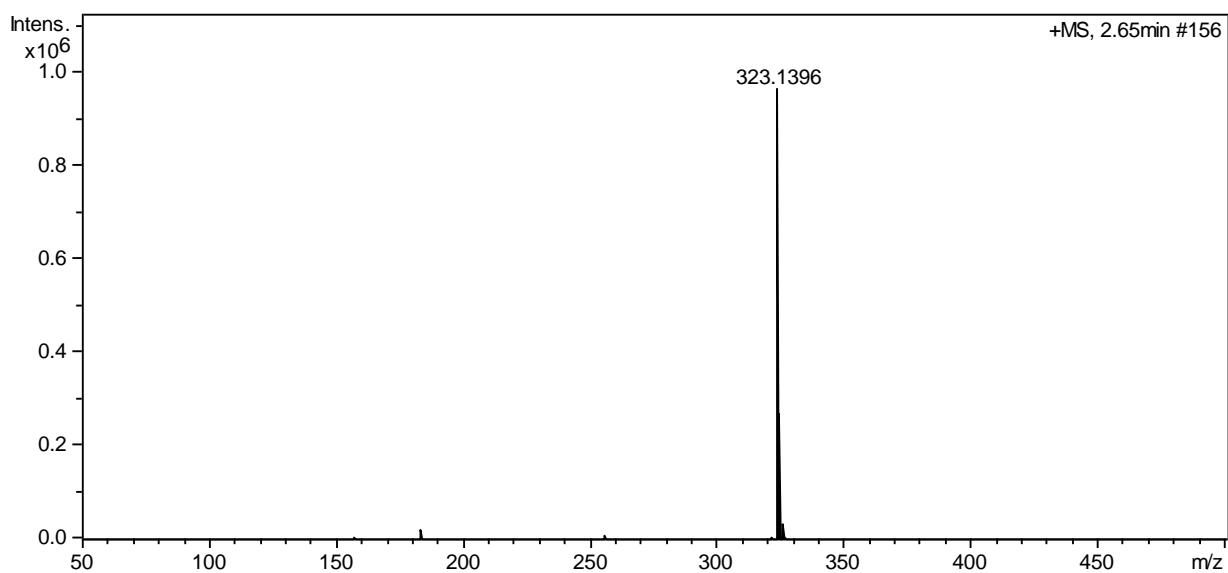


**Figure S6.** ESI-TOF HRMS spectrum of **AHB18**.

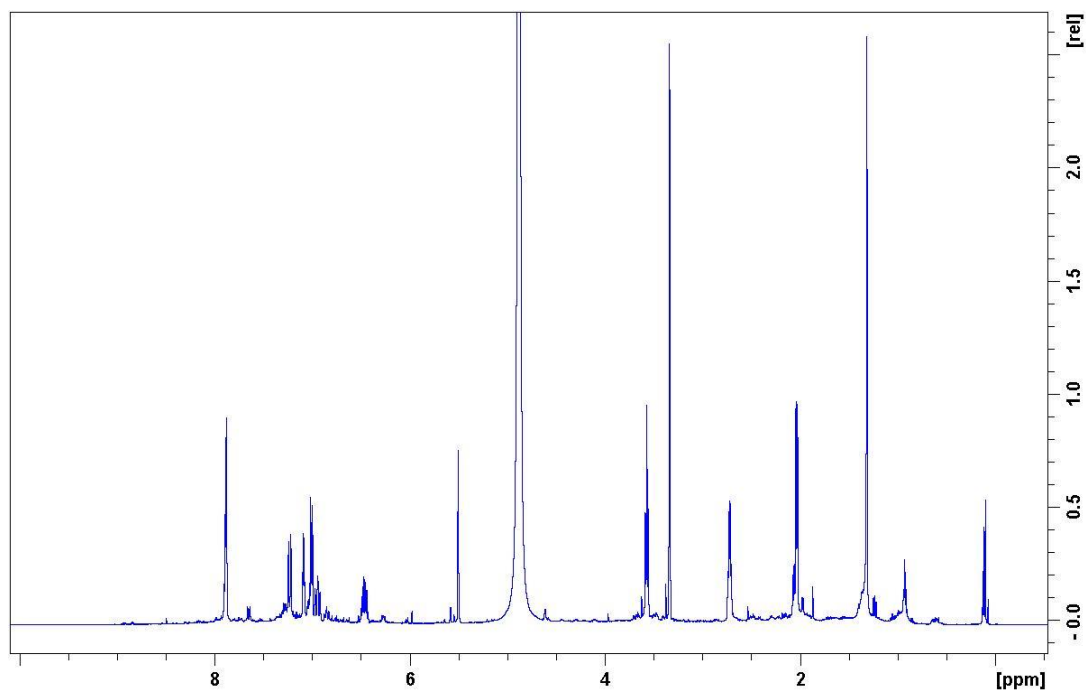


**Figure S7.**  $^1\text{H}$  spectrum of **AHB18** ( $\text{CD}_3\text{OD}$ , 24  $^\circ\text{C}$ , 500 MHz).

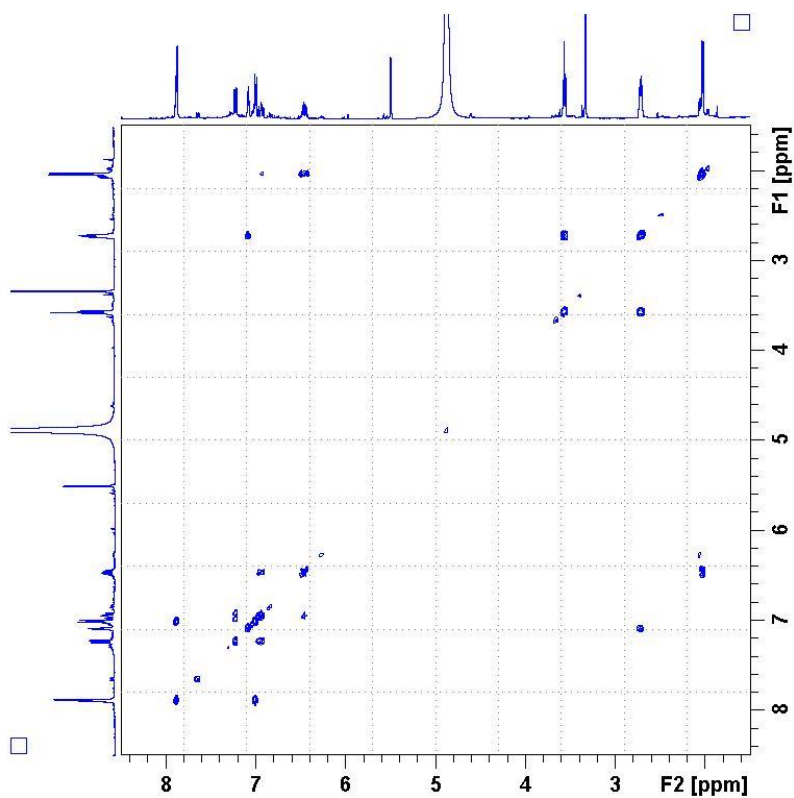


**Figure S8.** COSY spectrum of **AHB18**.

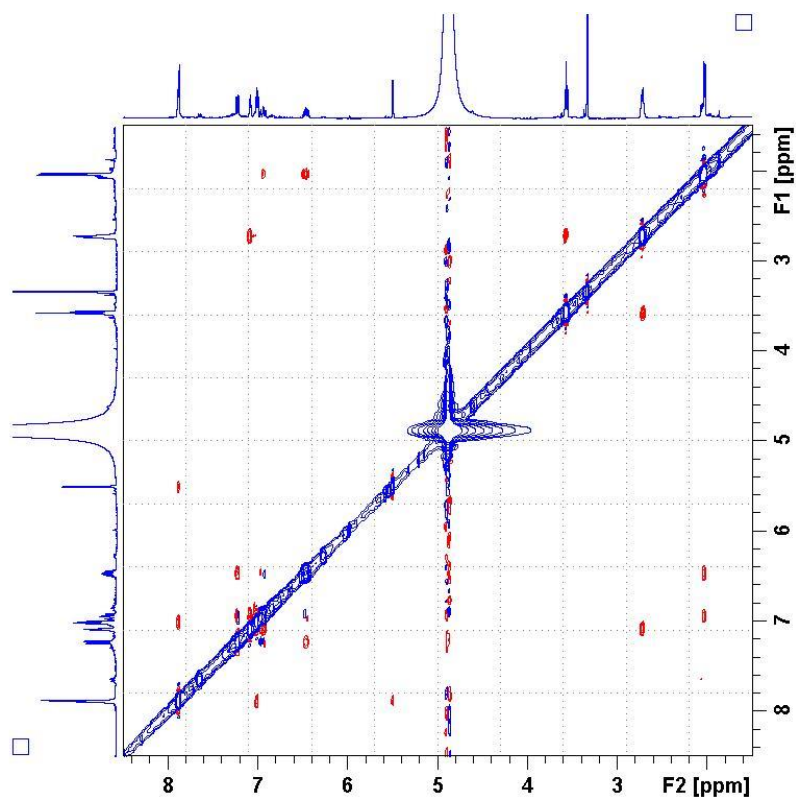


Figure S9. NOESY spectrum of **AHB18**.

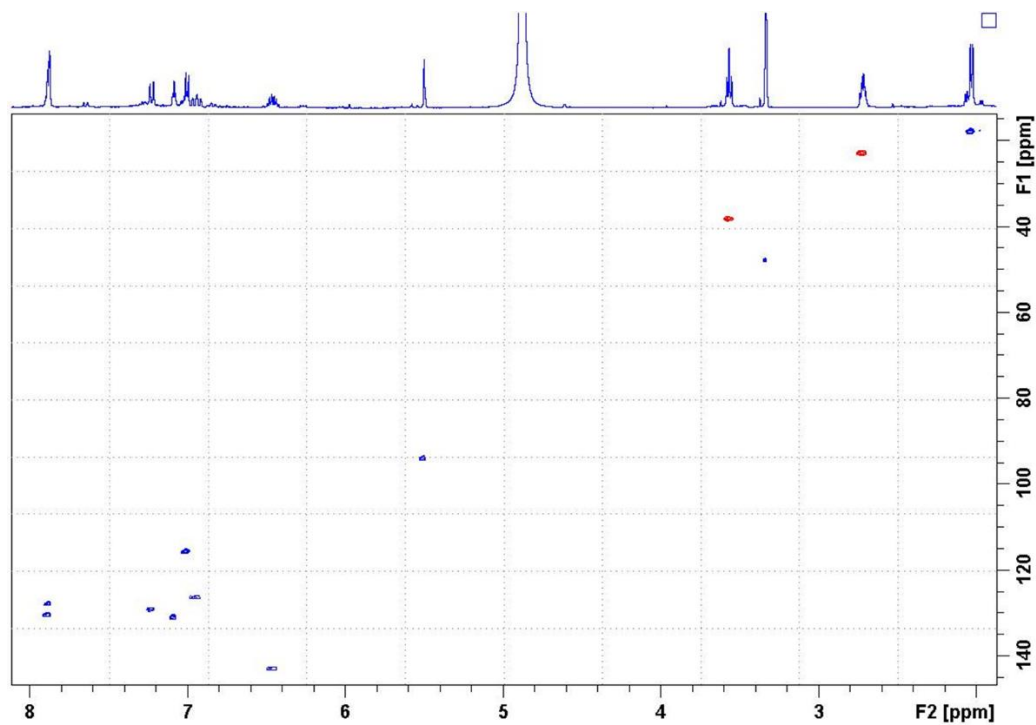
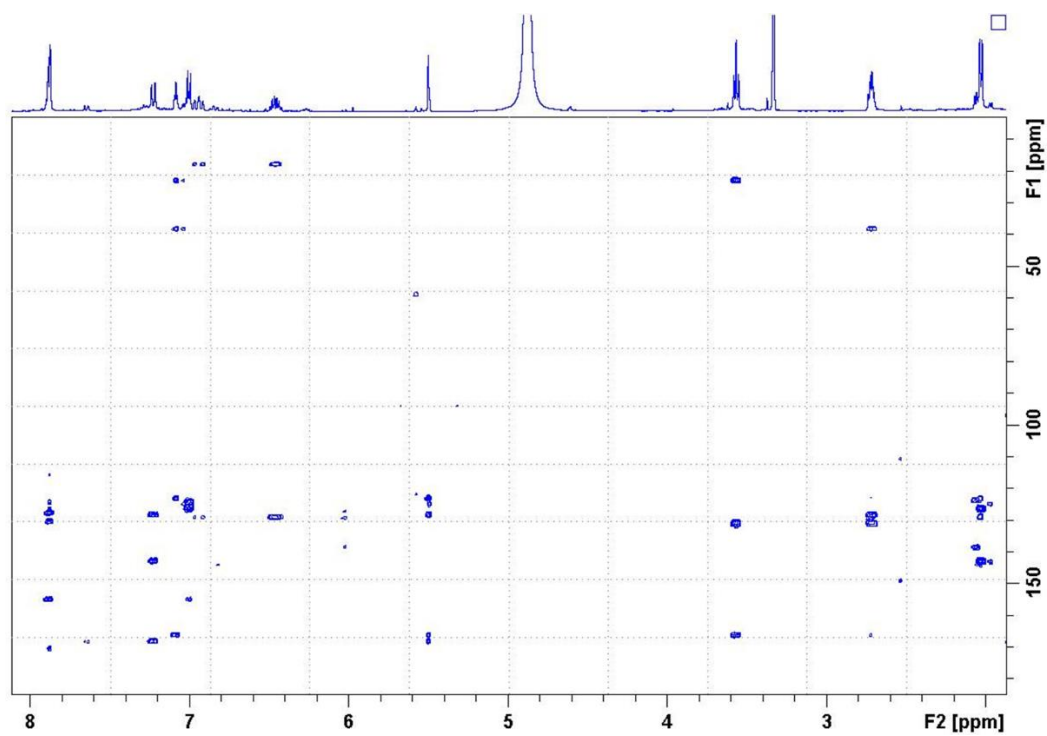
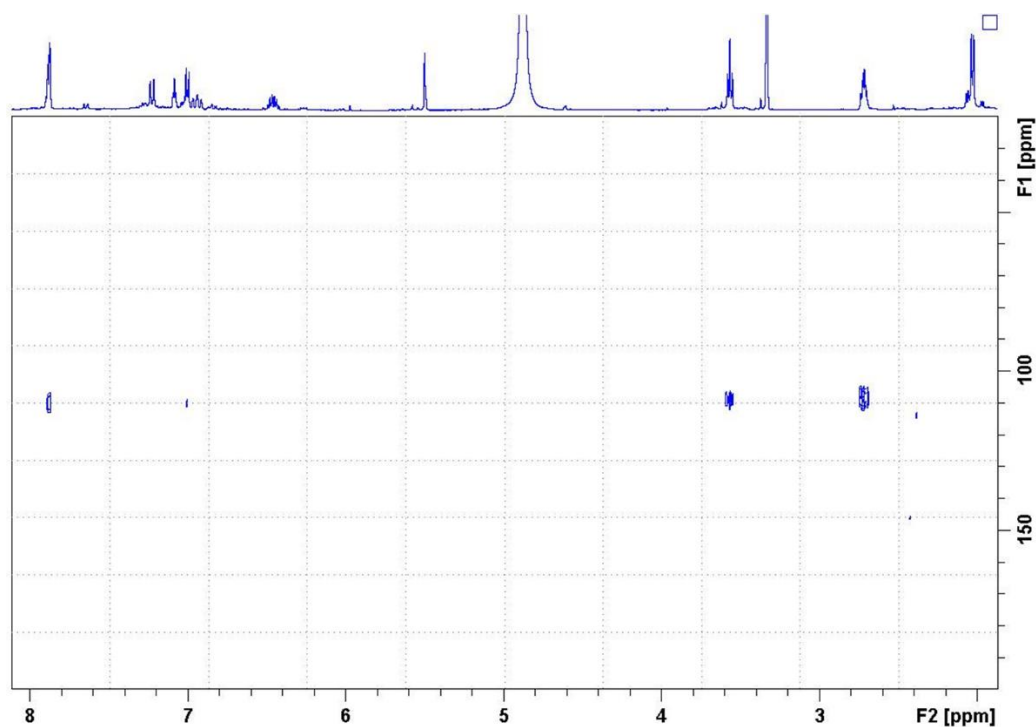


Figure S10. HSQC spectrum of **AHB18**.



**Figure S11.**  $^1\text{H}$ - $^{13}\text{C}$  HMBC spectrum of **AHB18**.



**Figure S12.**  $^1\text{H}$ - $^{15}\text{N}$  HMBC spectrum of **AHB18**.



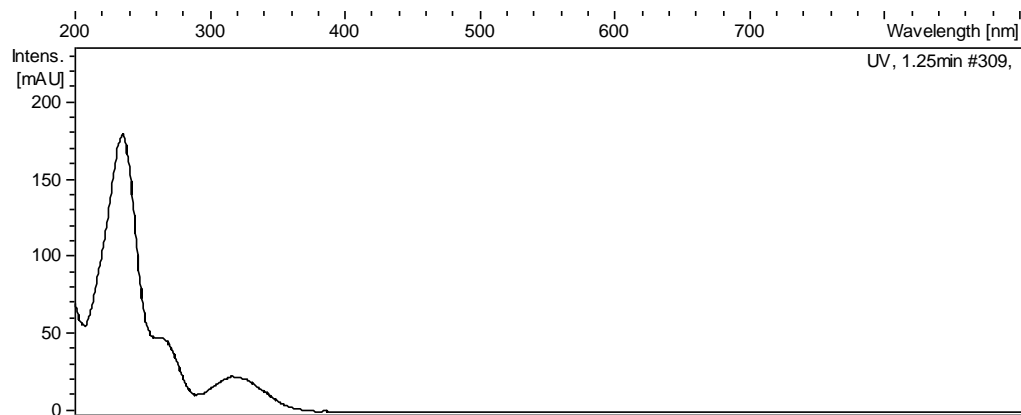


**Figure S13.** UV-vis (DAD) spectrum of **AHB74**.

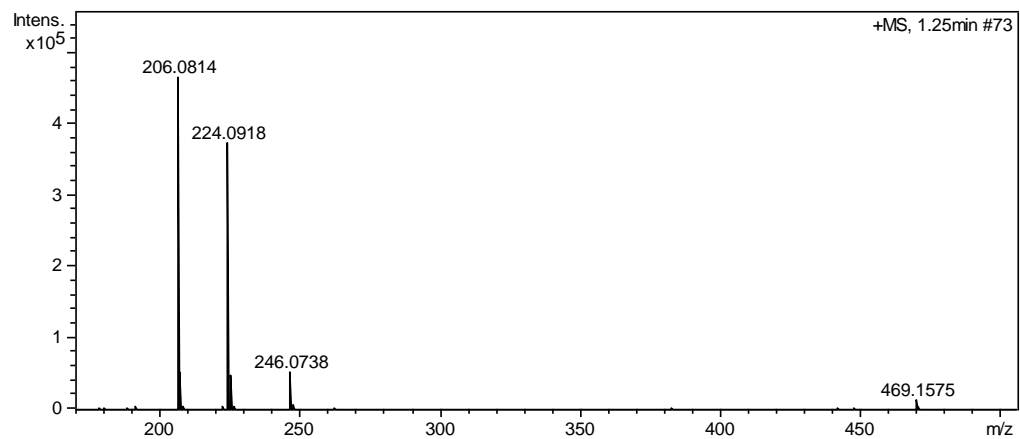


**Figure S14.** ESI-TOF HRMS spectrum of **AHB74**.

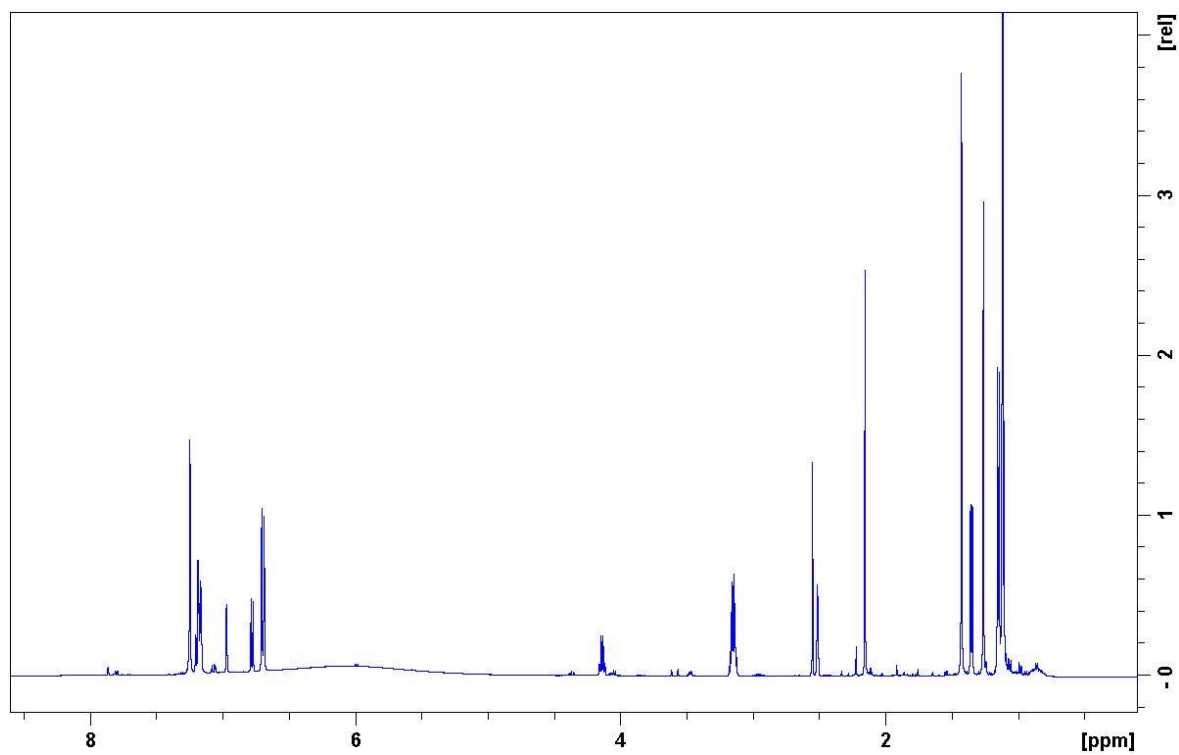


Figure S15.  $^1\text{H}$  spectrum of **AHB74** (DMSO- $\text{d}_6$ , 24 °C, 500 MHz).

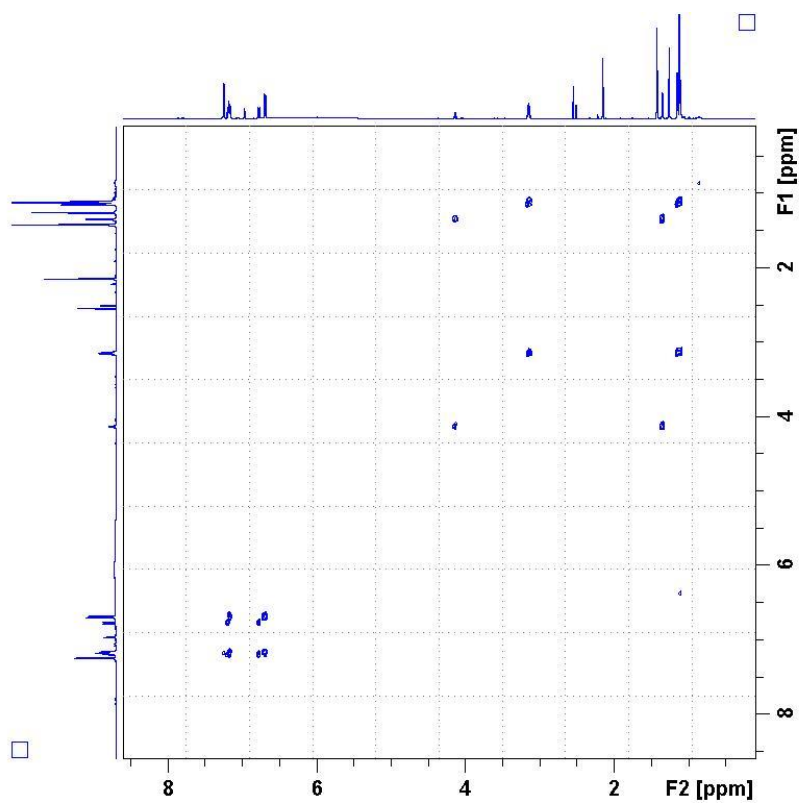


Figure S16. COSY spectrum of **AHB74**.

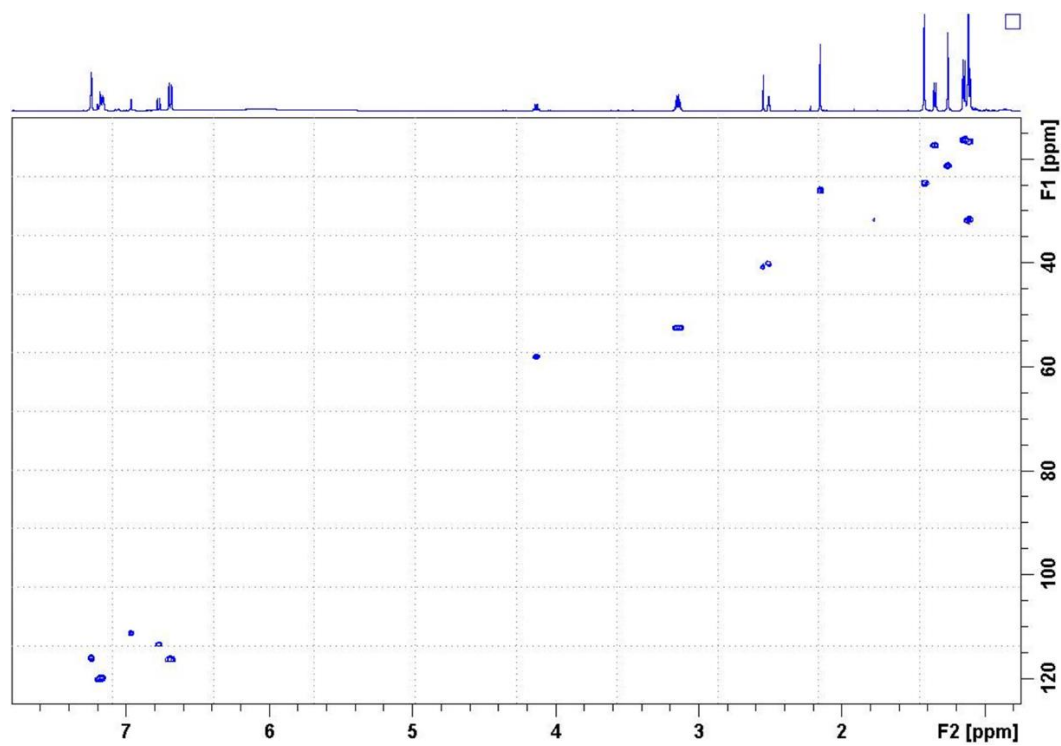


Figure S17. HSQC spectrum of AHB74.

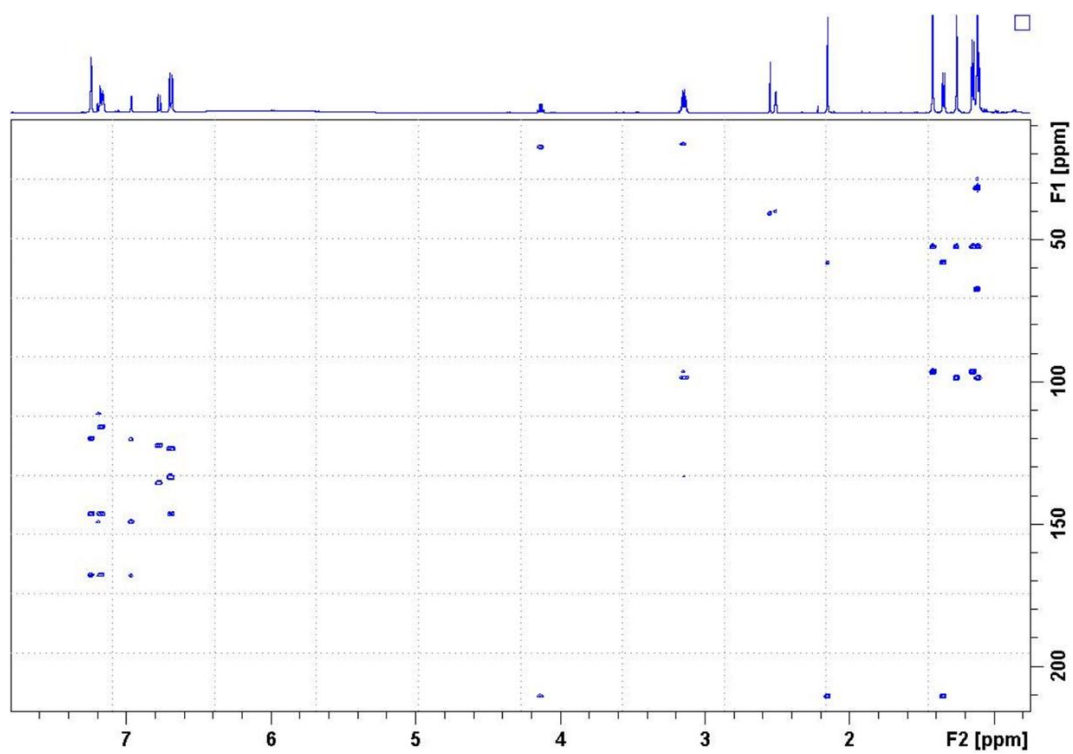
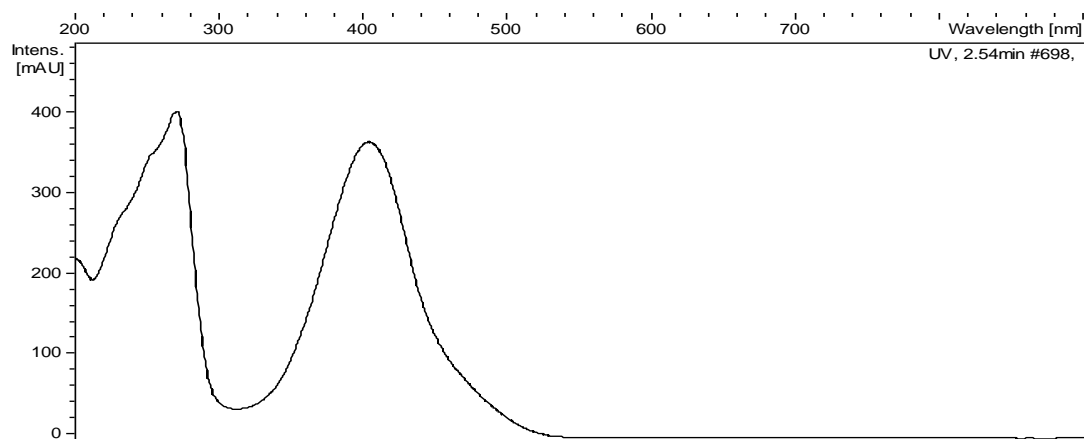
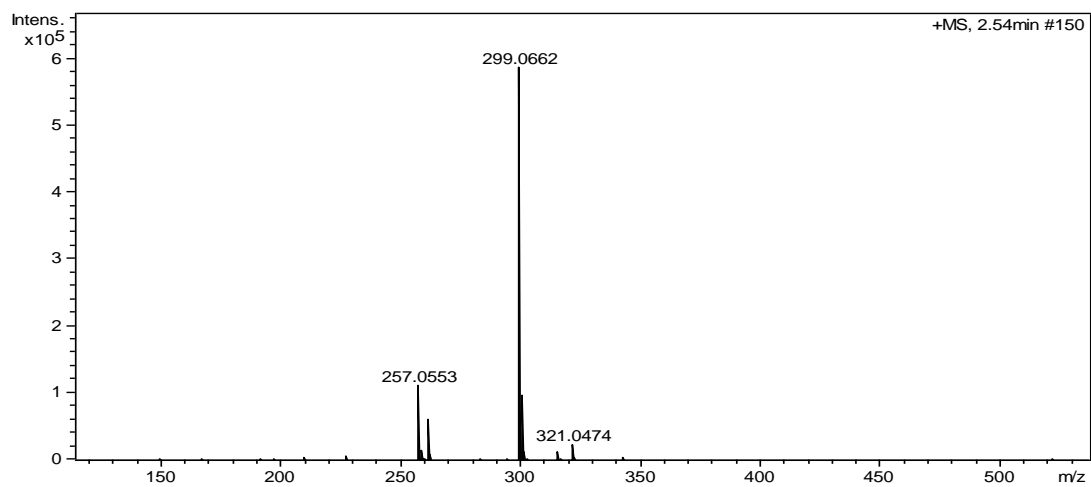


Figure S18. HMBC spectrum of AHB74.



**Figure S19.** UV-vis (DAD) spectrum of **AHB75**.



**Figure S20.** ESI-TOF HRMS spectrum of **AHB75**.

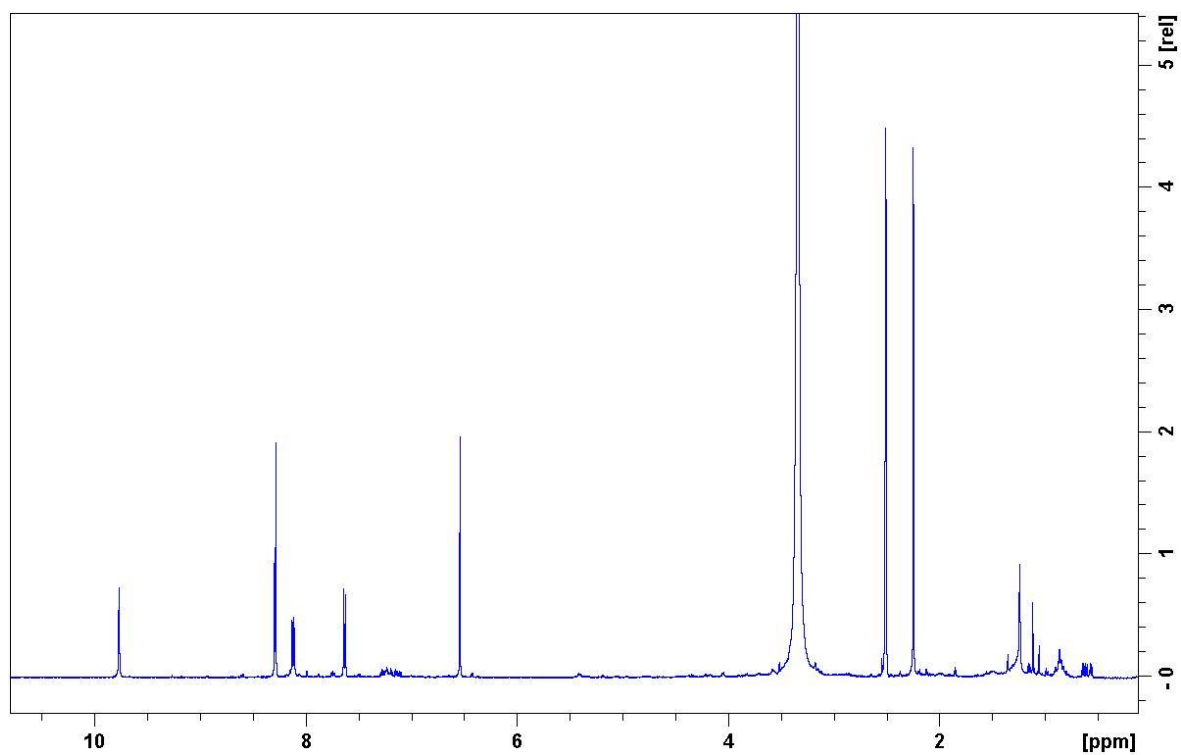


Figure S21.  $^1\text{H}$  spectrum of **AHB75** (DMSO- $d_6$ , 24 °C, 500 MHz).

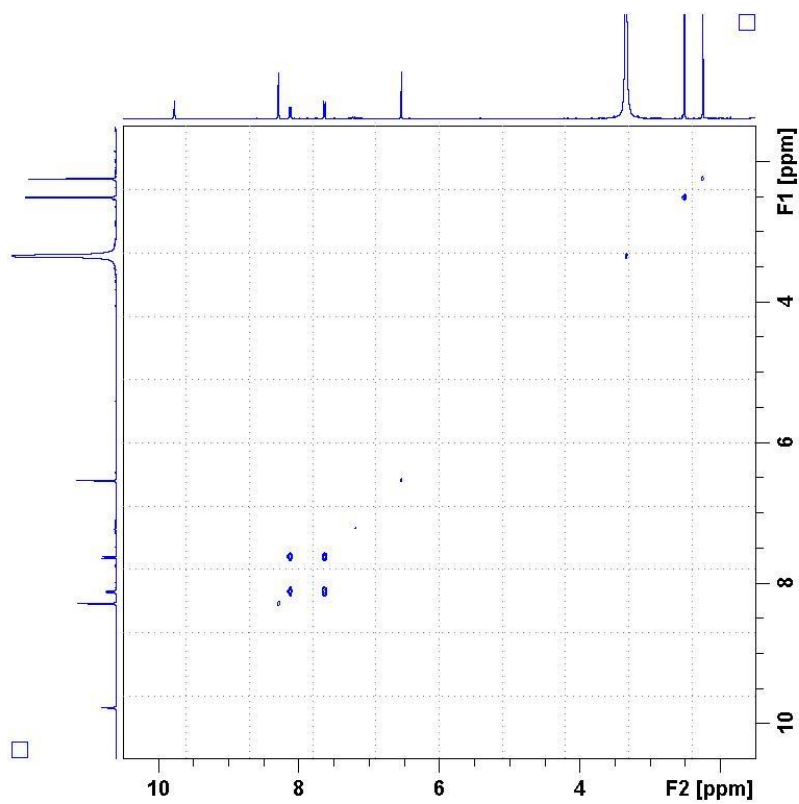


Figure S22. COSY spectrum of **AHB75**.

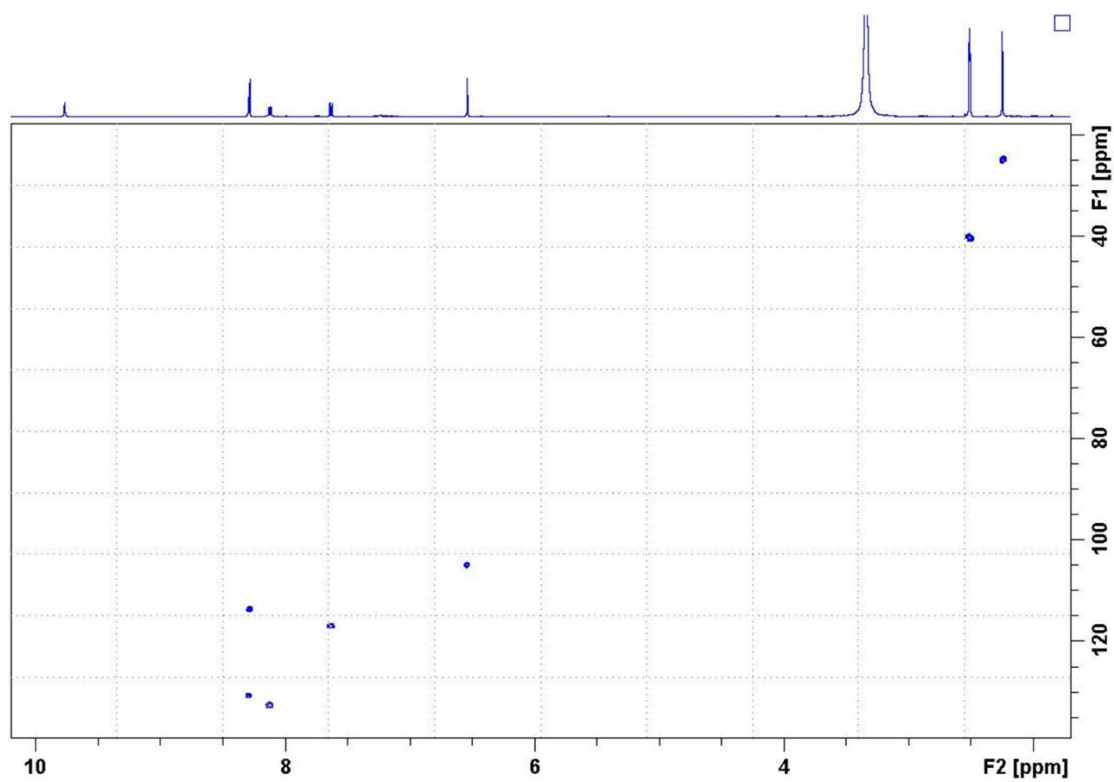


Figure S23. HSQC spectrum of **AHB75**.

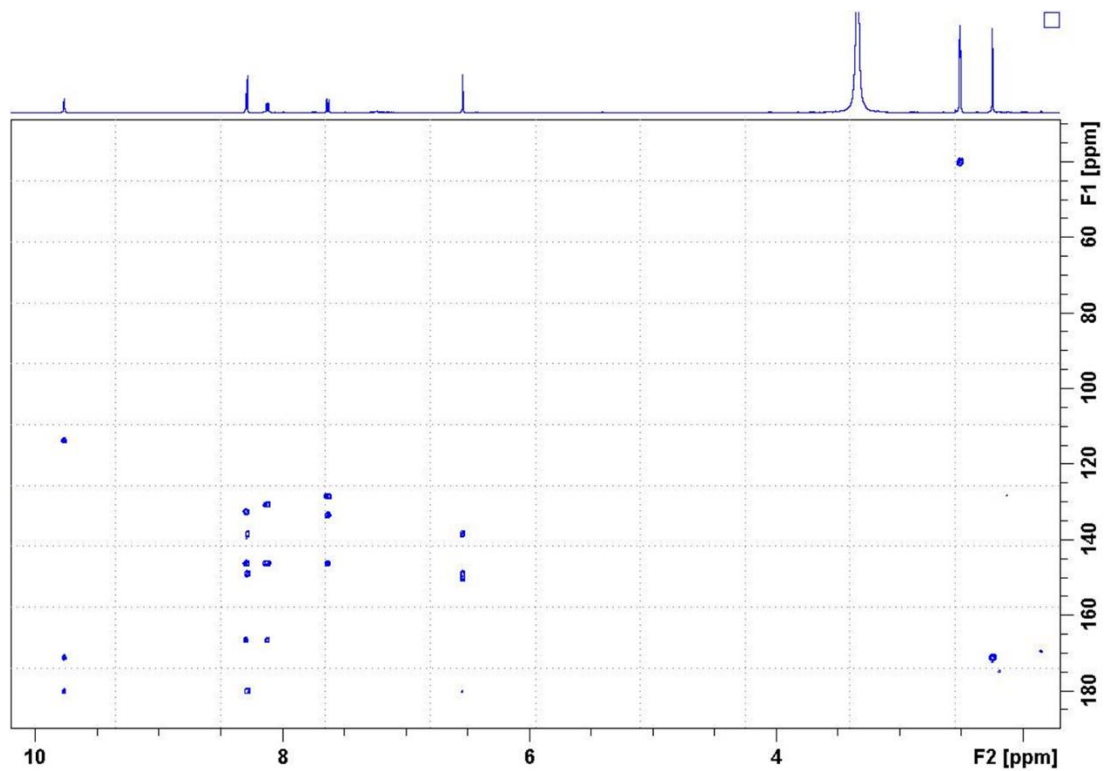
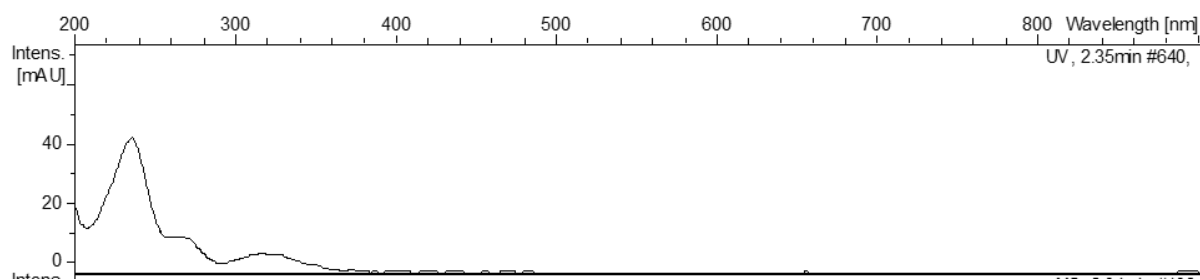
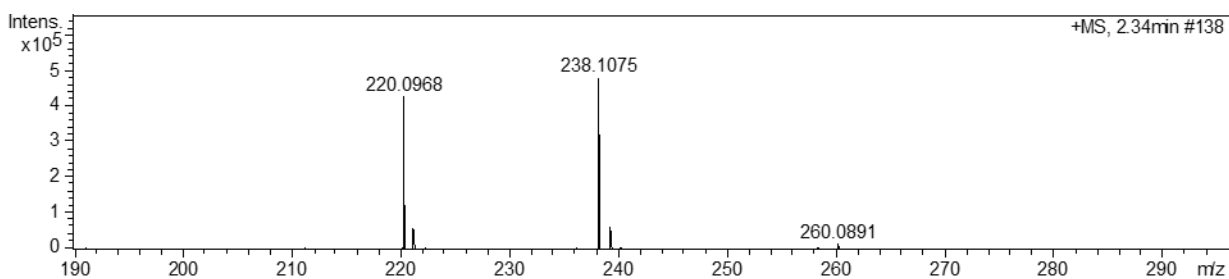


Figure S24. HMBC spectrum of **AHB75**.



**Figure S25.** UV-vis (DAD) spectrum of **AHB76**.



**Figure S26.** ESI-TOF HRMS spectrum of **AHB76**.

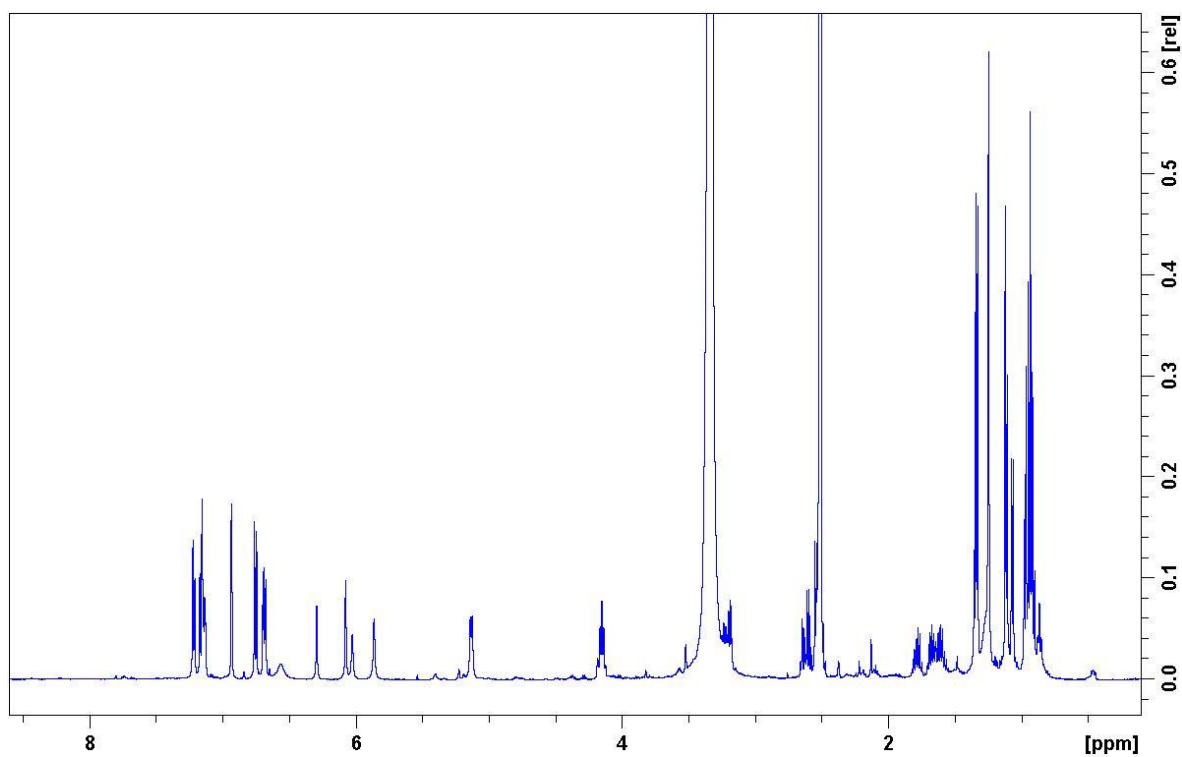


Figure 7  $^1\text{H}$  spectrum of **AHB76** (DMSO- $d_6$ , 24 °C, 500 MHz).

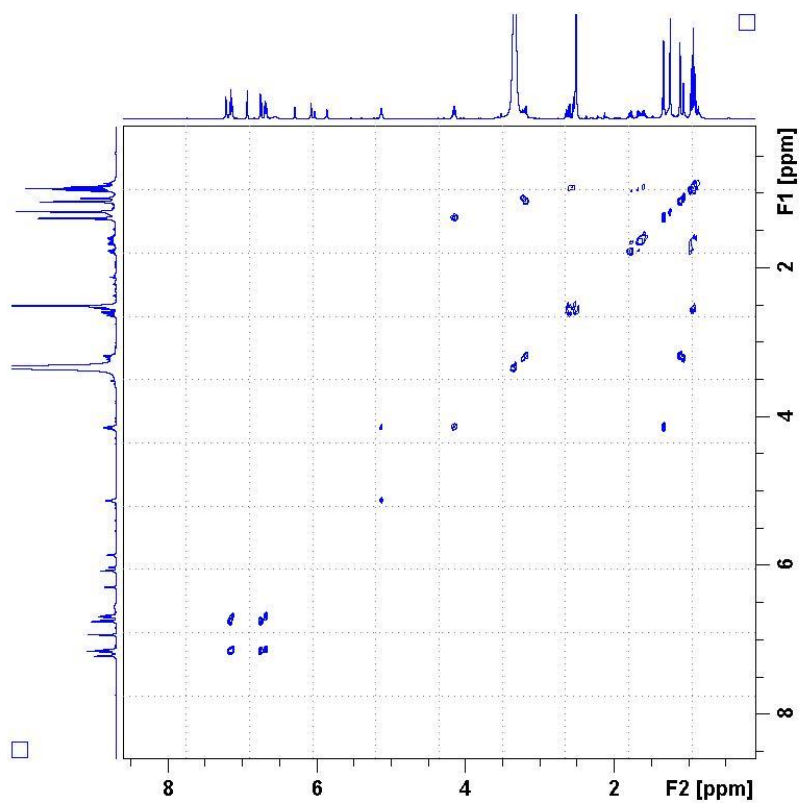


Figure S28. COSY spectrum of **AHB76**.



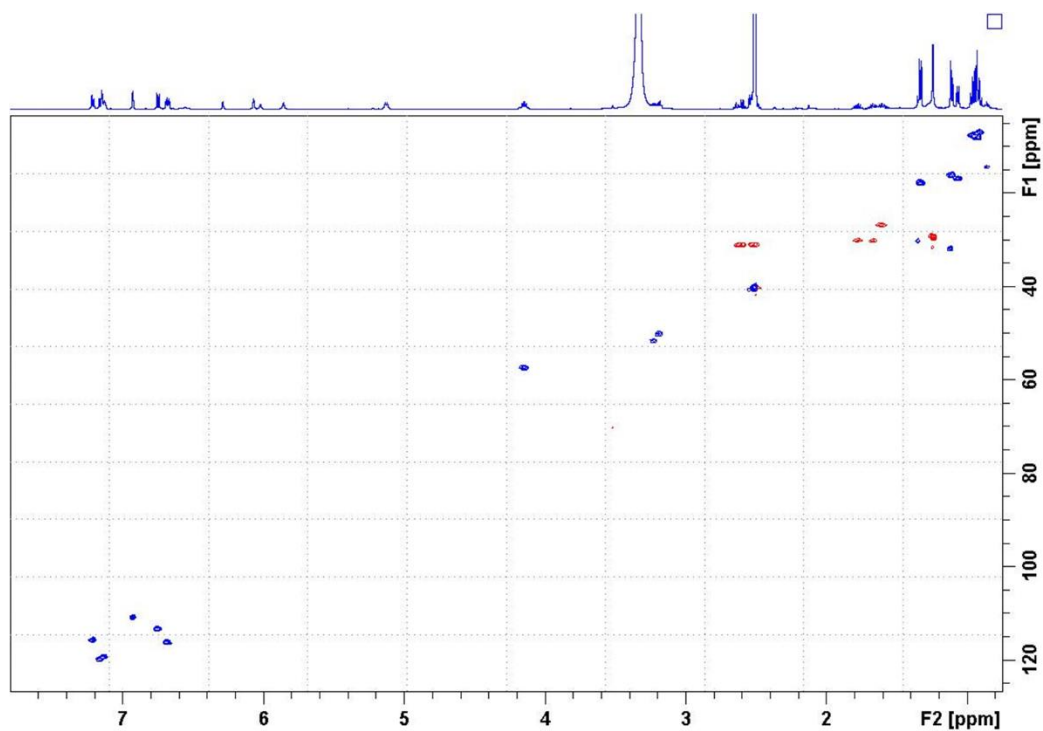


Figure S29. HSQC spectrum of **AHB76**.

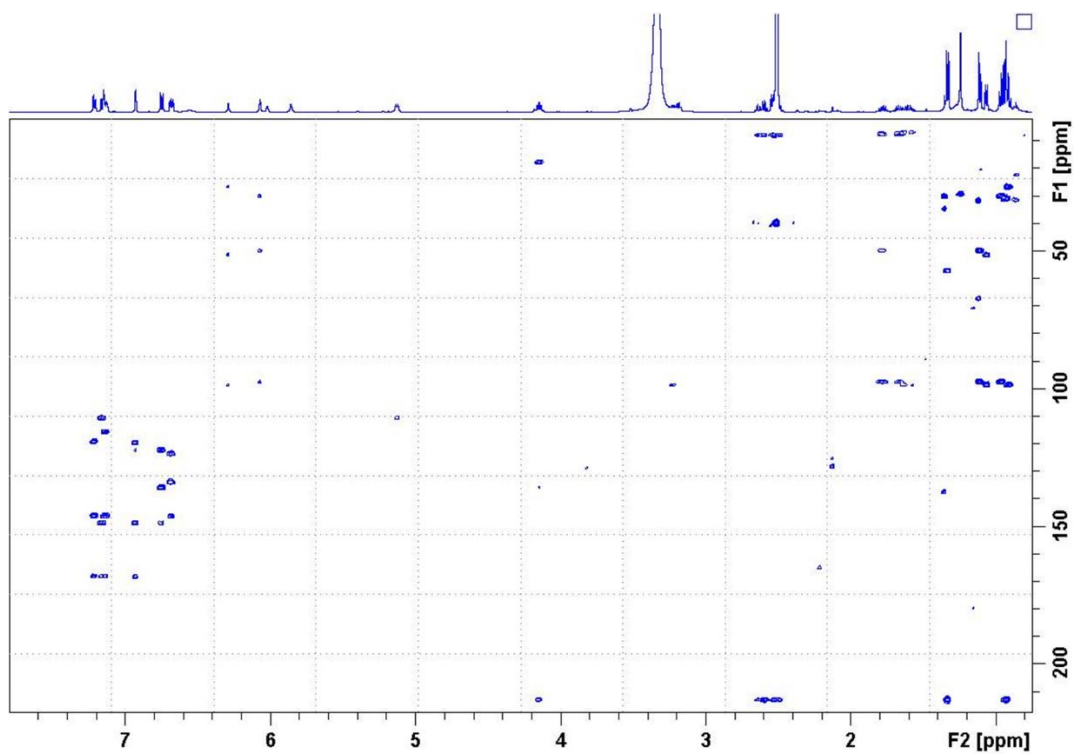


Figure S309. HMBC spectrum of **AHB76**.

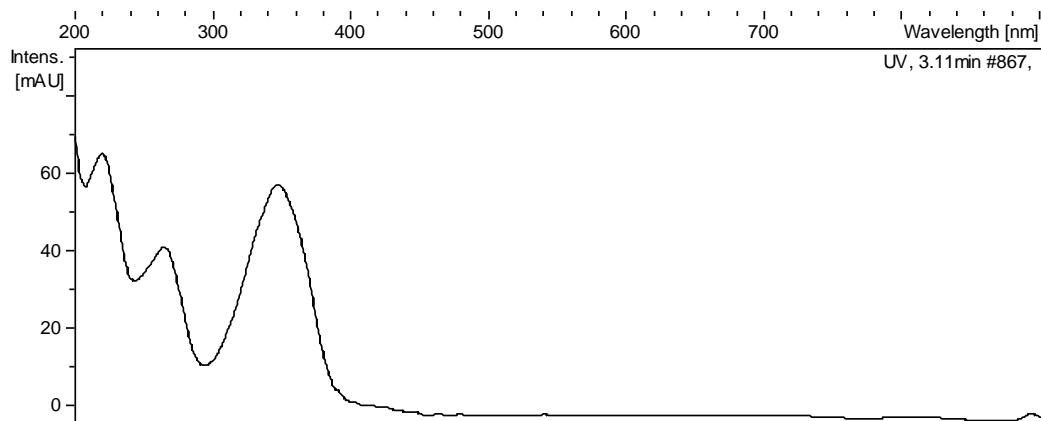


Figure S31. UV-vis (DAD) spectrum of **AHB77**.

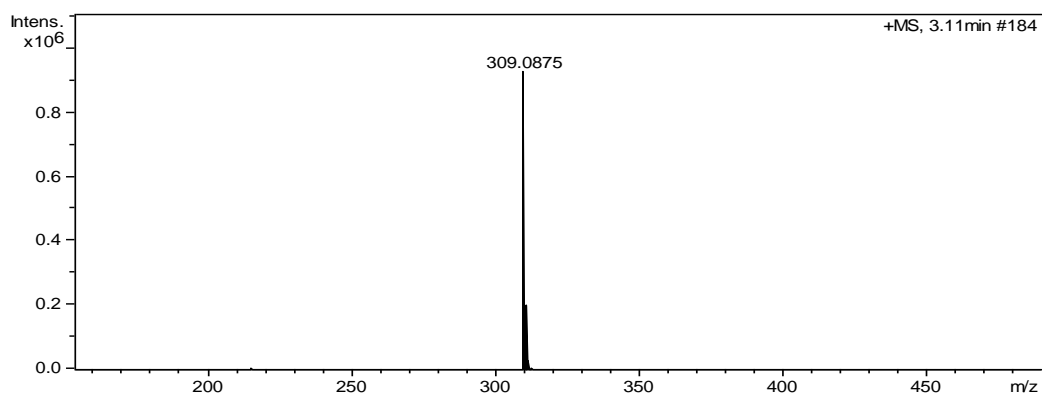


Figure S32. ESI-TOF HRMS spectrum of **AHB77**.

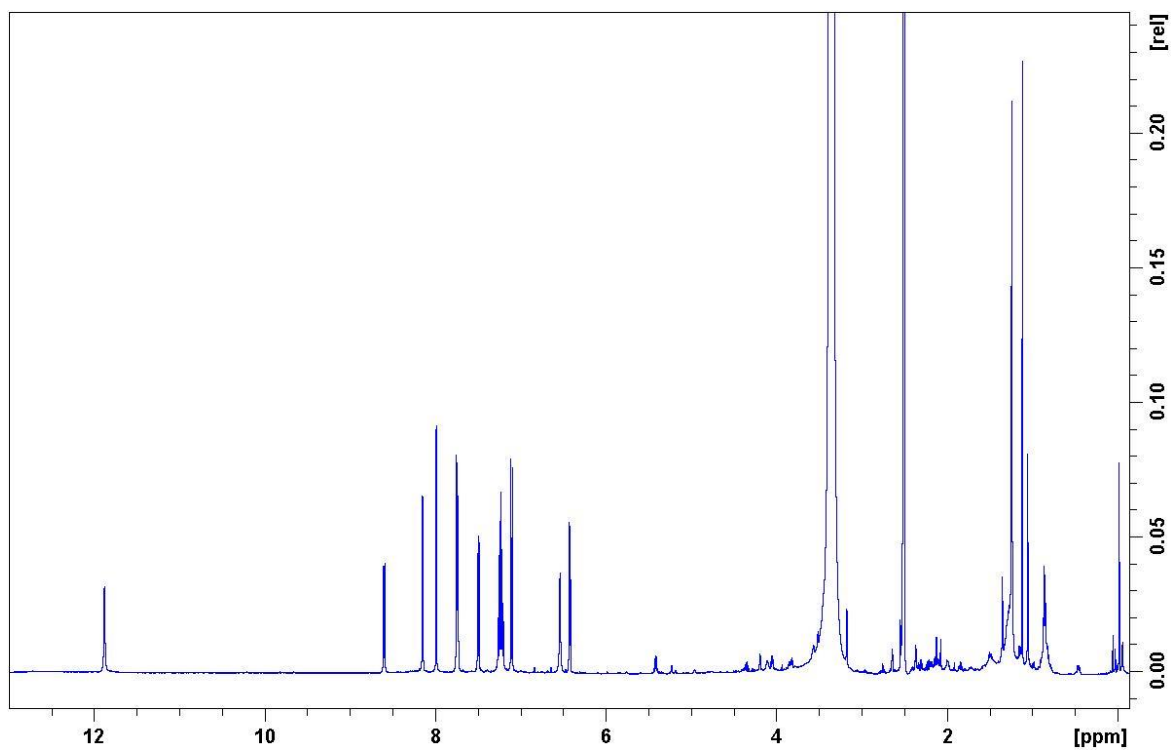


Figure S33.  $^1\text{H}$  spectrum of **AHB77** (DMSO- $d_6$ , 24 °C, 500 MHz).

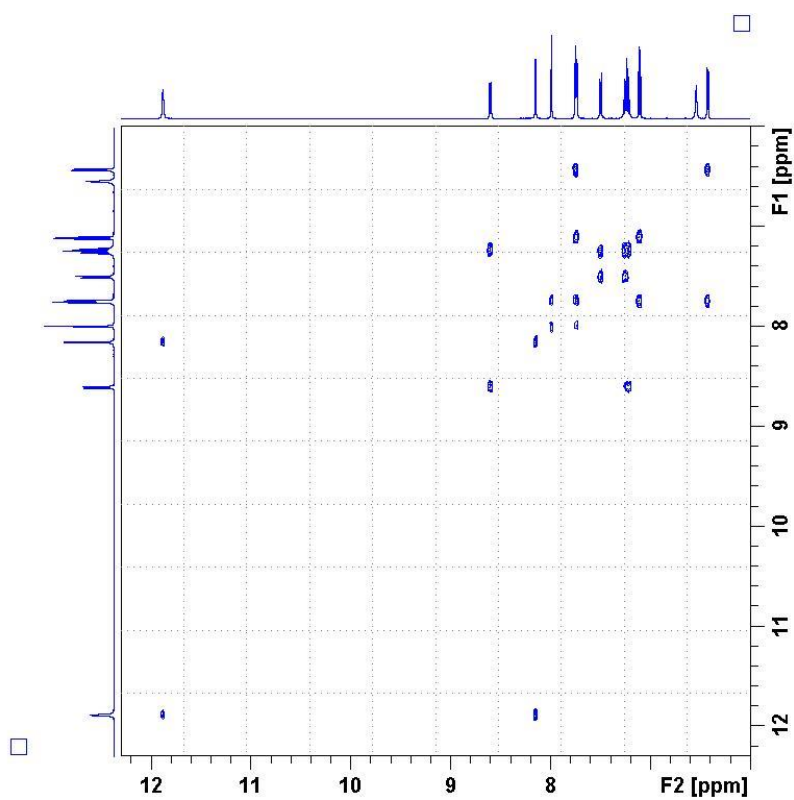


Figure S34. COSY spectrum of **AHB77**.

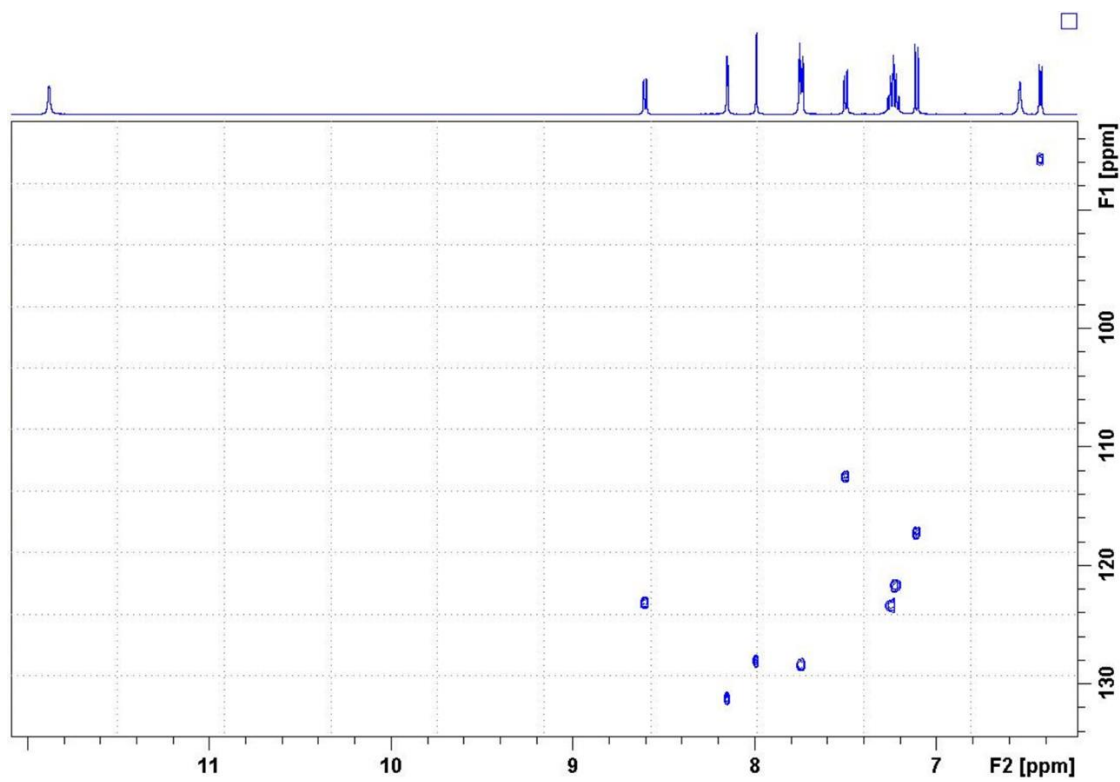


Figure S35. HSQC spectrum of **AHB77**.

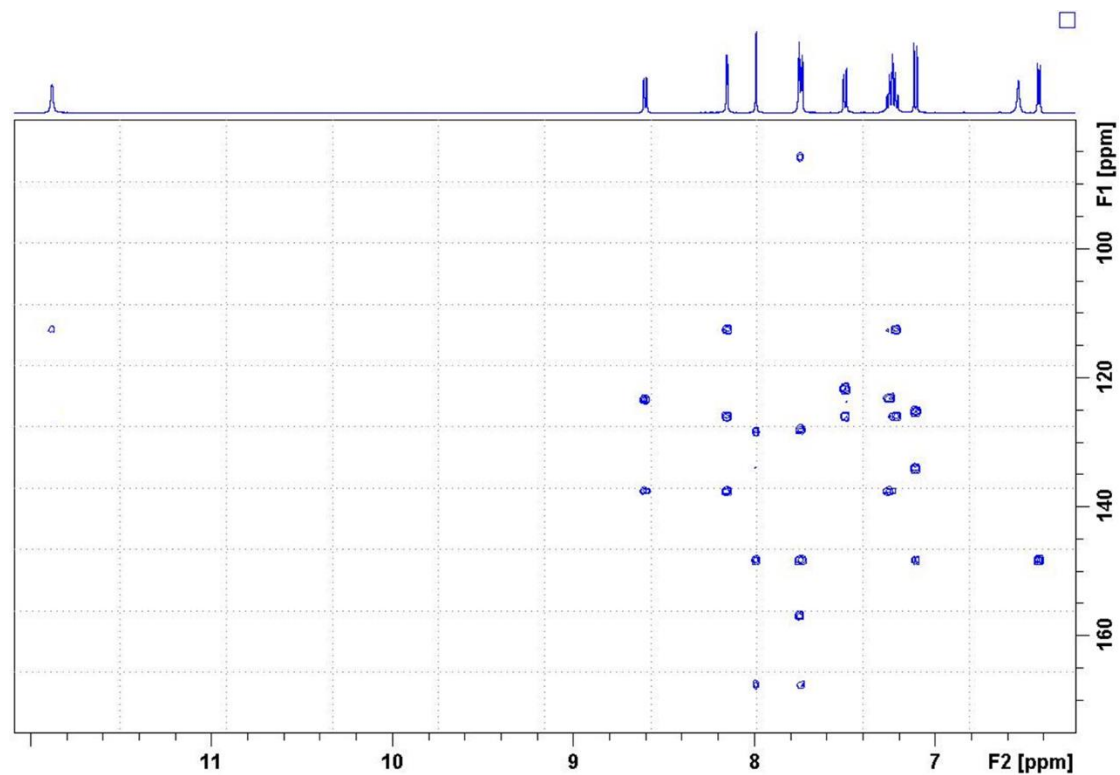
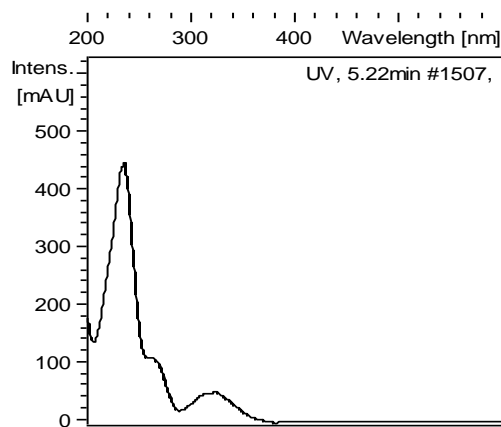
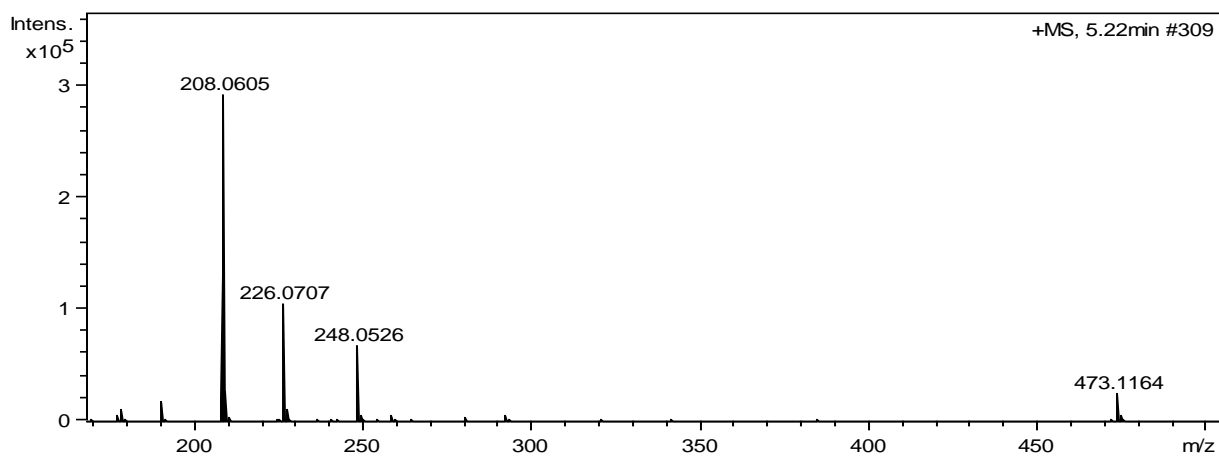


Figure S36. HMBC spectrum of **AHB77**.



**Figure S37.** UV-vis (DAD) spectrum of **AHB118**.



**Figure S38.** ESI-TOF HRMS spectrum of **AHB118**.

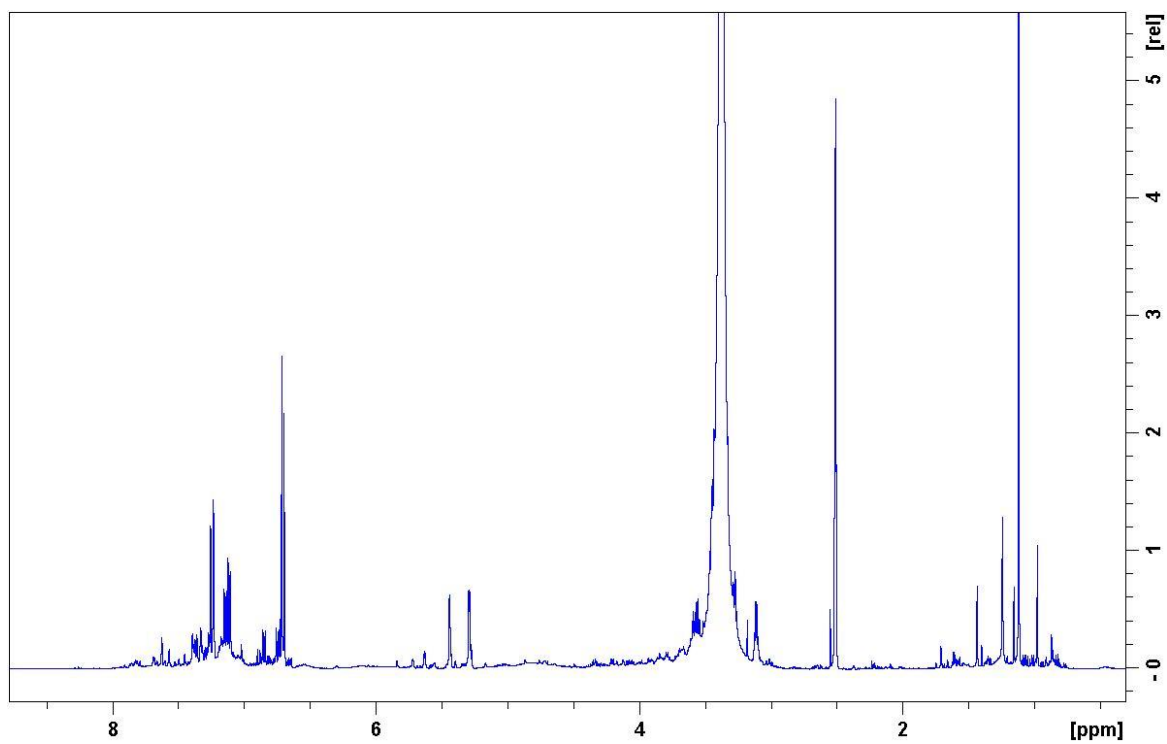


Figure S39.  $^1\text{H}$  spectrum of **AHB118** (DMSO- $\text{d}_6$ , 24 °C, 500 MHz).

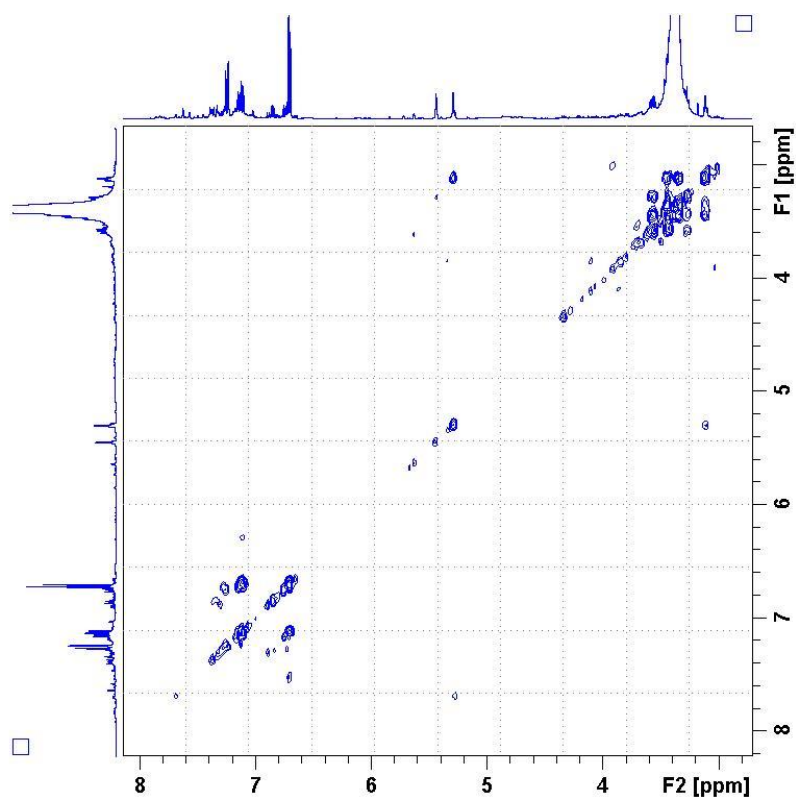


Figure S40. COSY spectrum of **AHB118**.

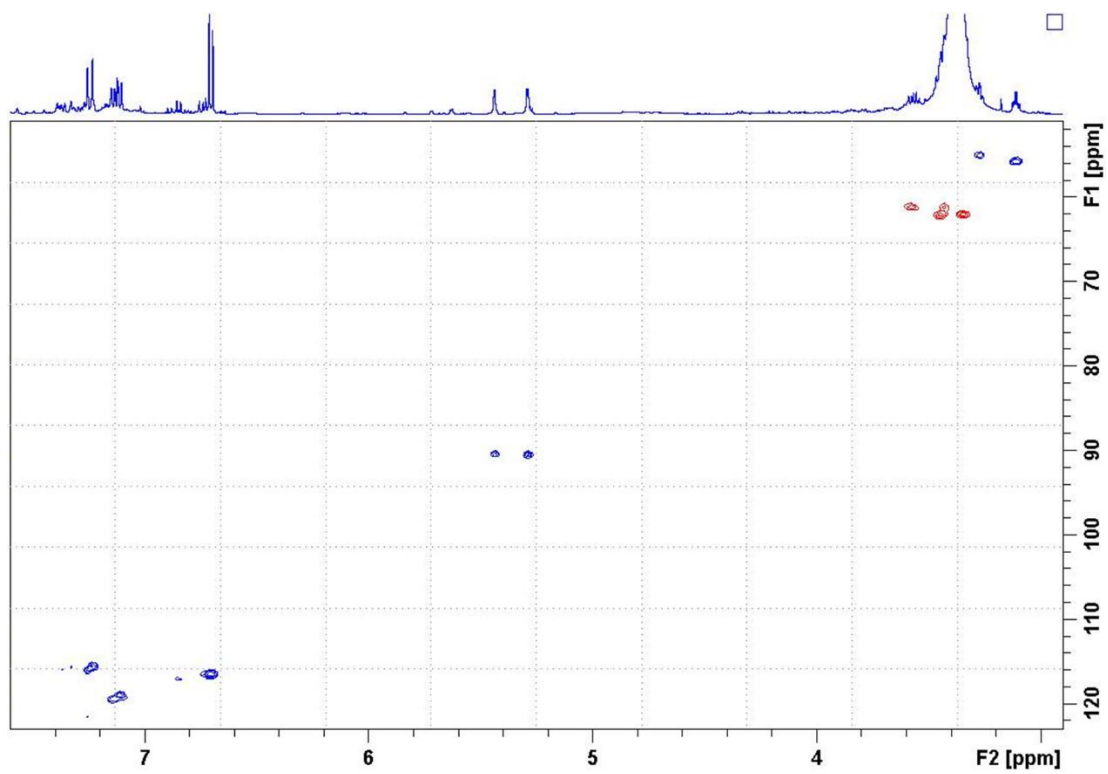


Figure S41. HSQC spectrum of AHB118.

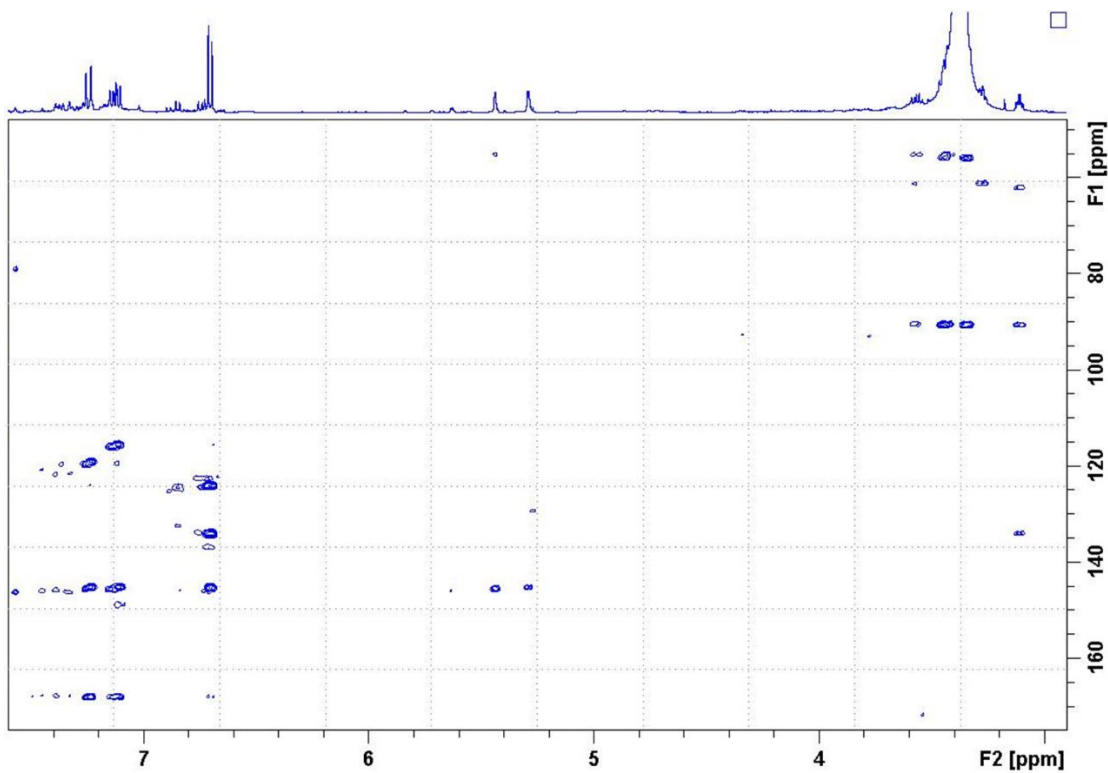
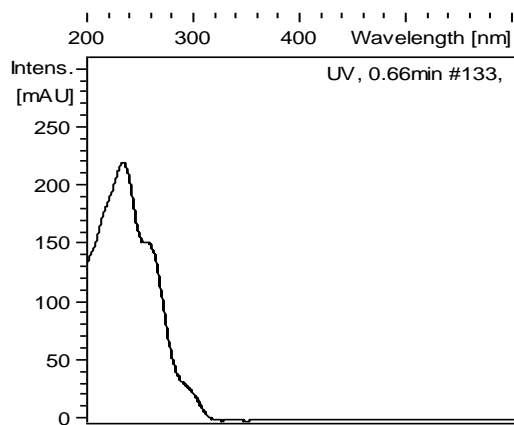
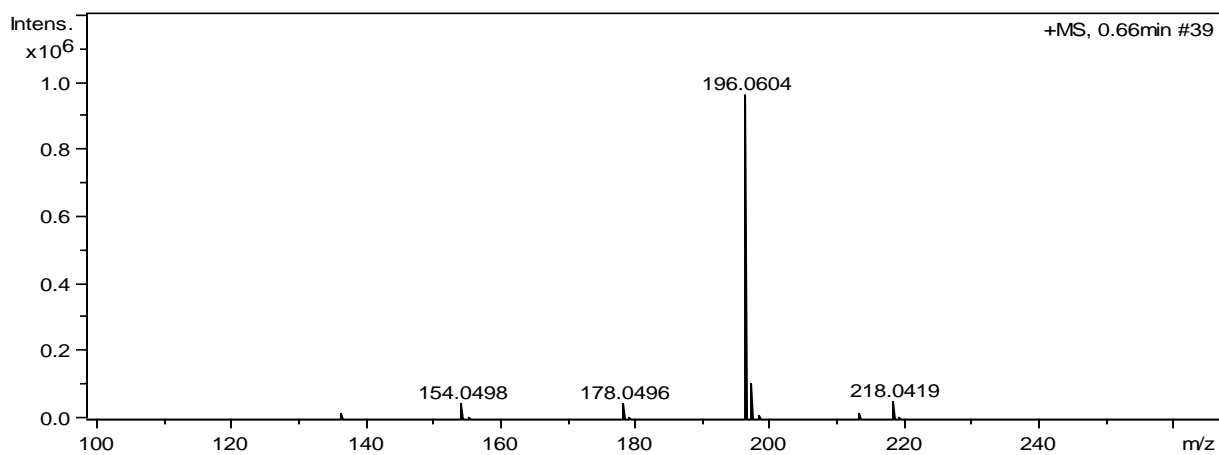


Figure S42. HMBC spectrum of AHB118.



**Figure S43.** UV-vis (DAD) spectrum of **AHB119**.



**Figure S44.** ESI-TOF HRMS spectrum of **AHB119**.



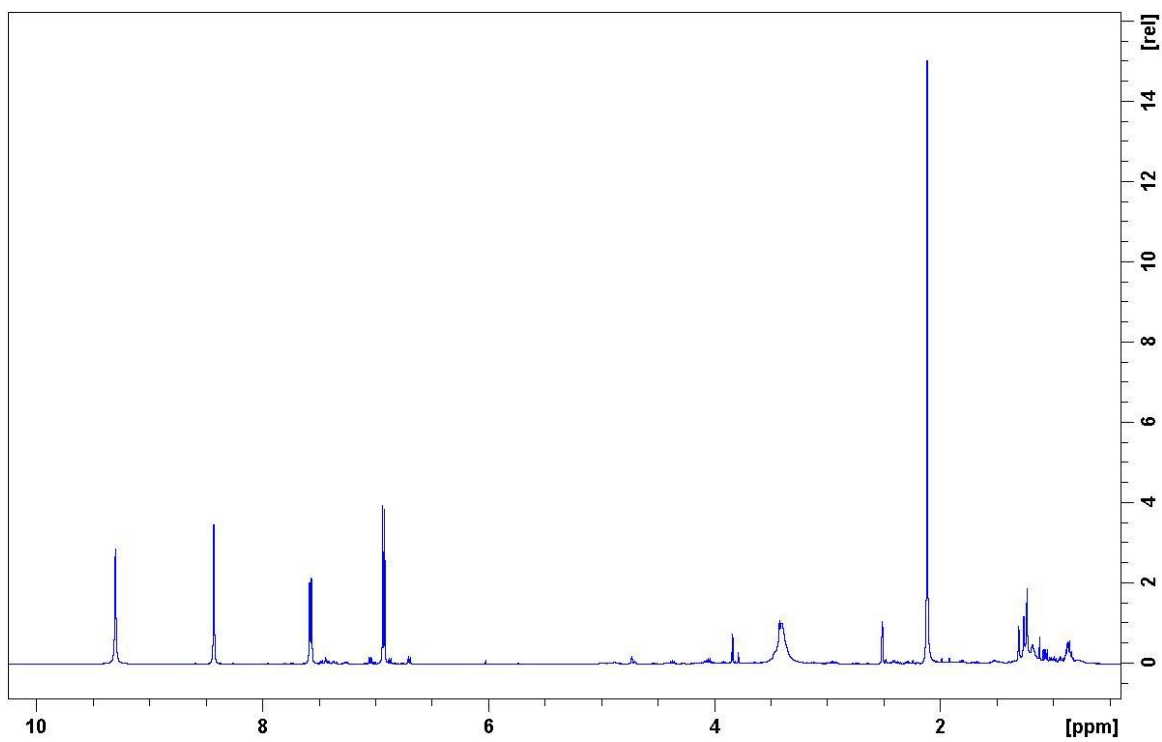


Figure S45.  $^1\text{H}$  spectrum of **AHB119** (DMSO- $d_6$ , 24 °C, 500 MHz).

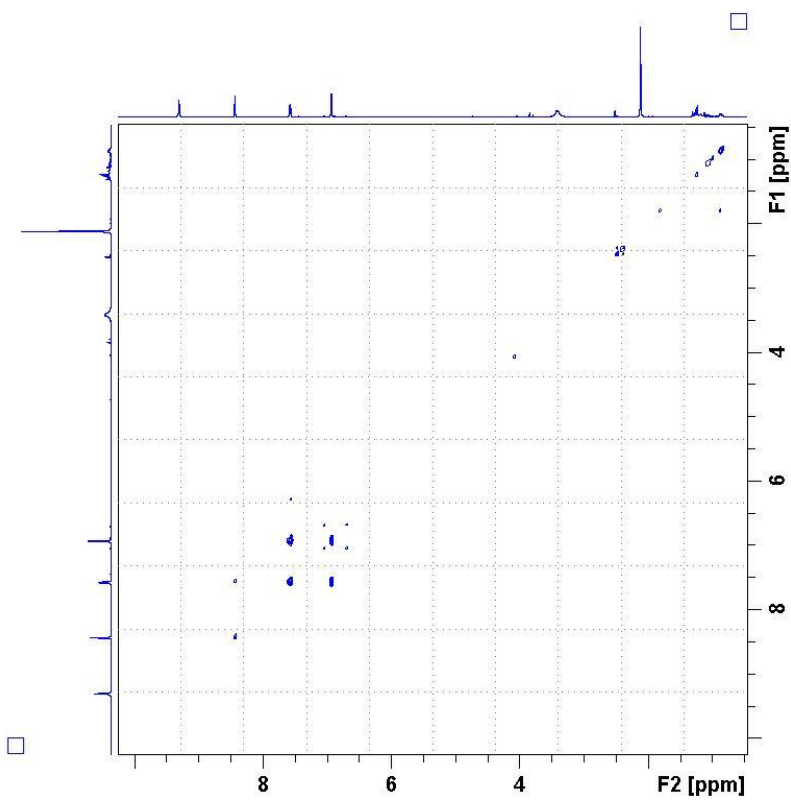


Figure S46. COSY spectrum of **AHB119**.

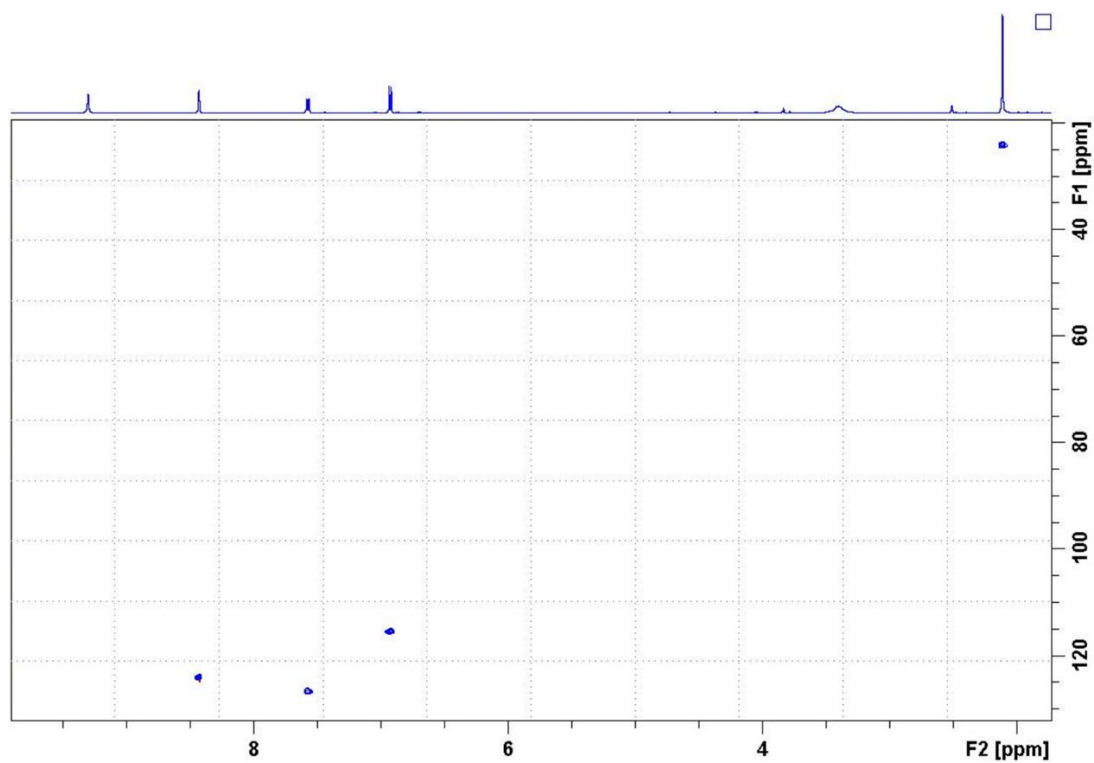


Figure S47. HSQC spectrum of AHB119.

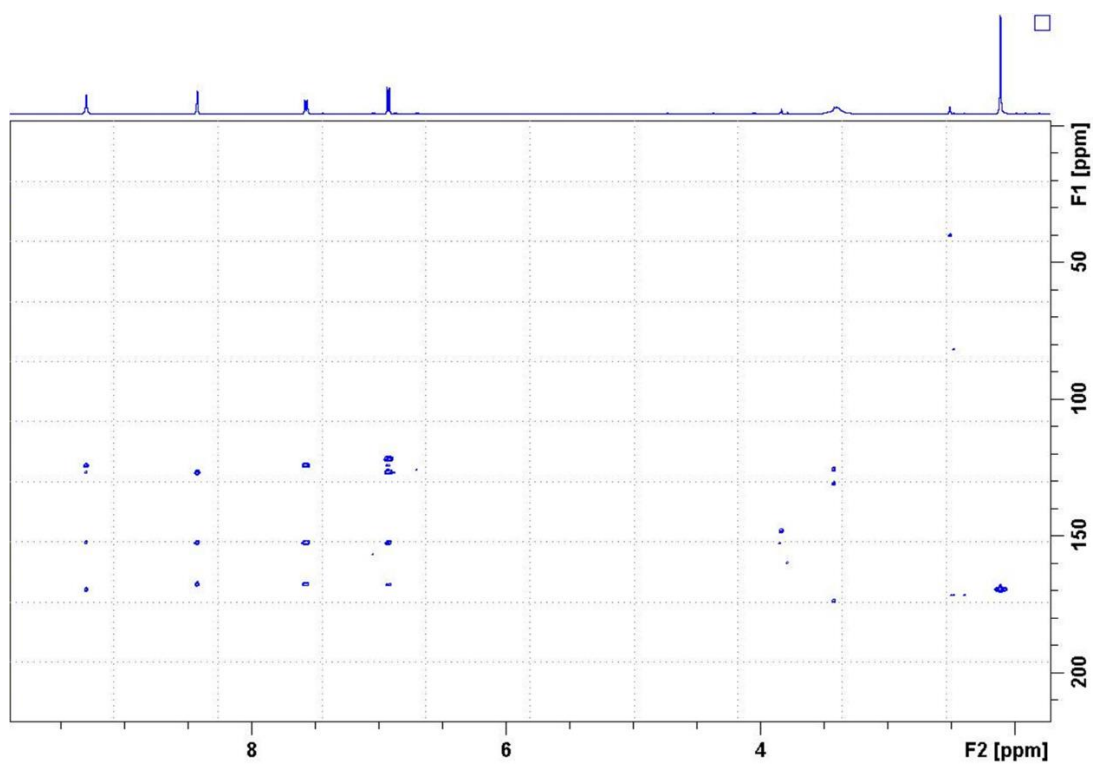
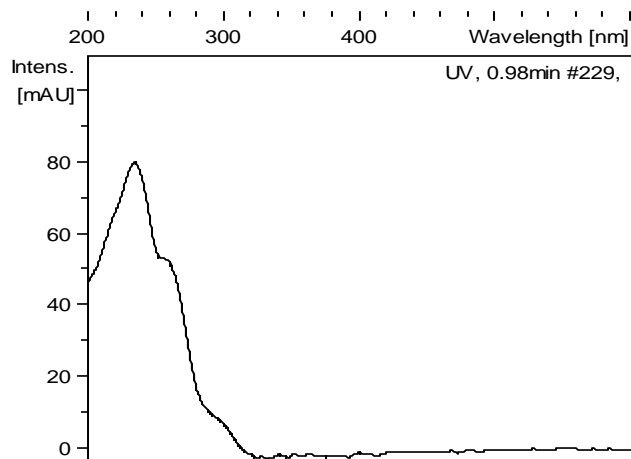
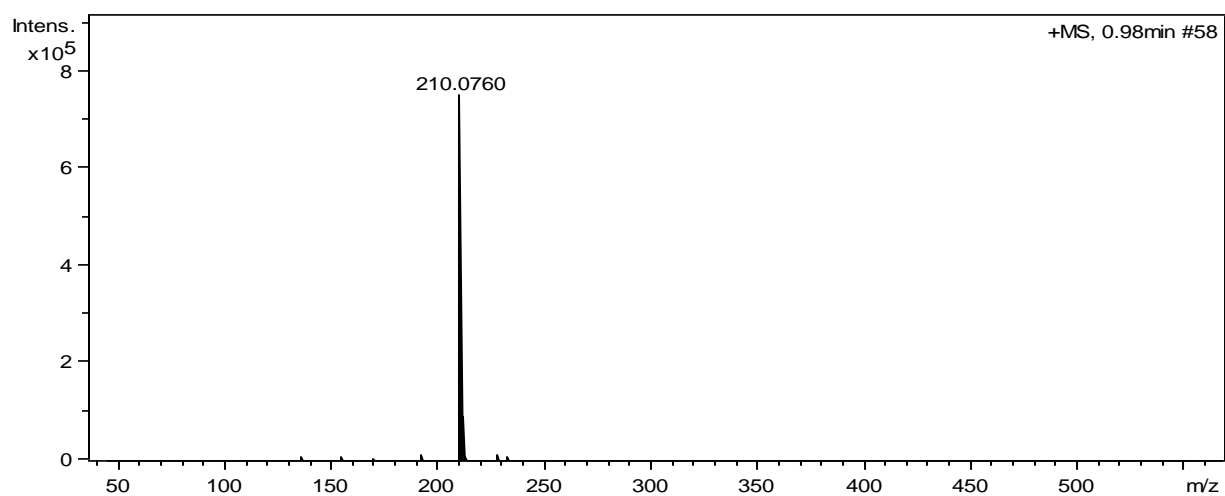


Figure S48. HMBC spectrum of AHB119.



**Figure S49.** UV-vis (DAD) spectrum of **AHB120**.



**Figure S50.** ESI-TOF HRMS spectrum of **AHB120**.

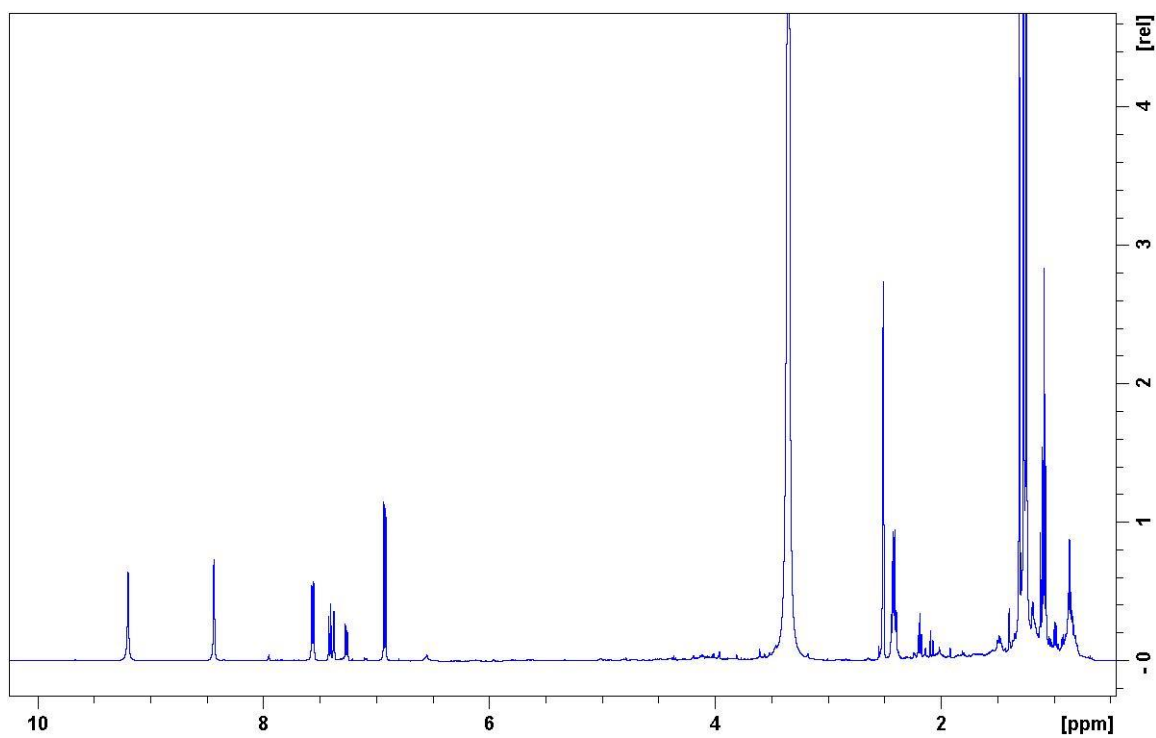


Figure S51.  $^1\text{H}$  spectrum of **AHB120** (DMSO- $d_6$ , 24 °C, 500 MHz).

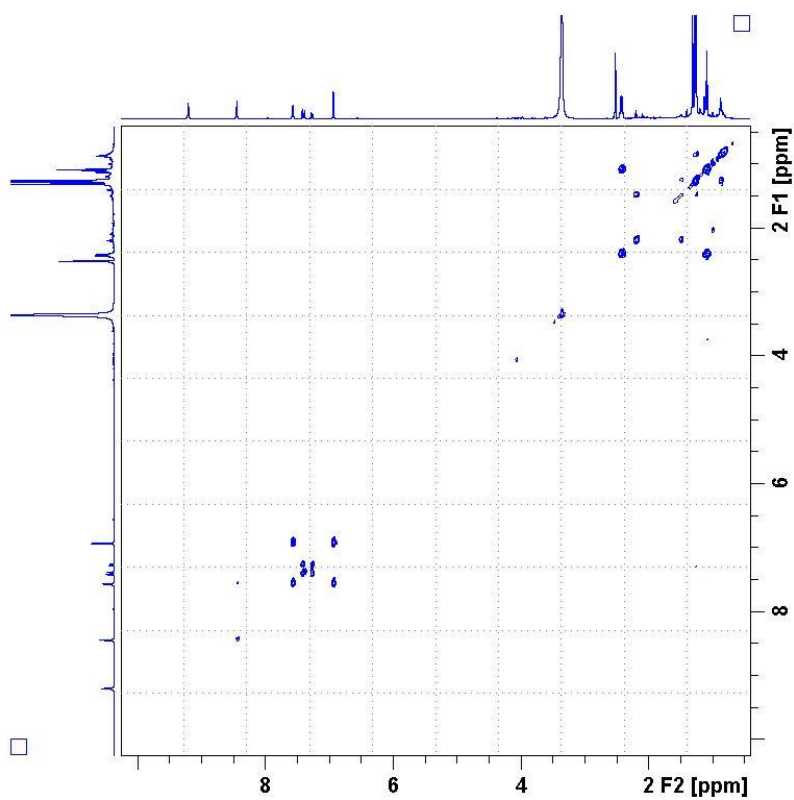


Figure S52. COSY spectrum of **AHB120**.

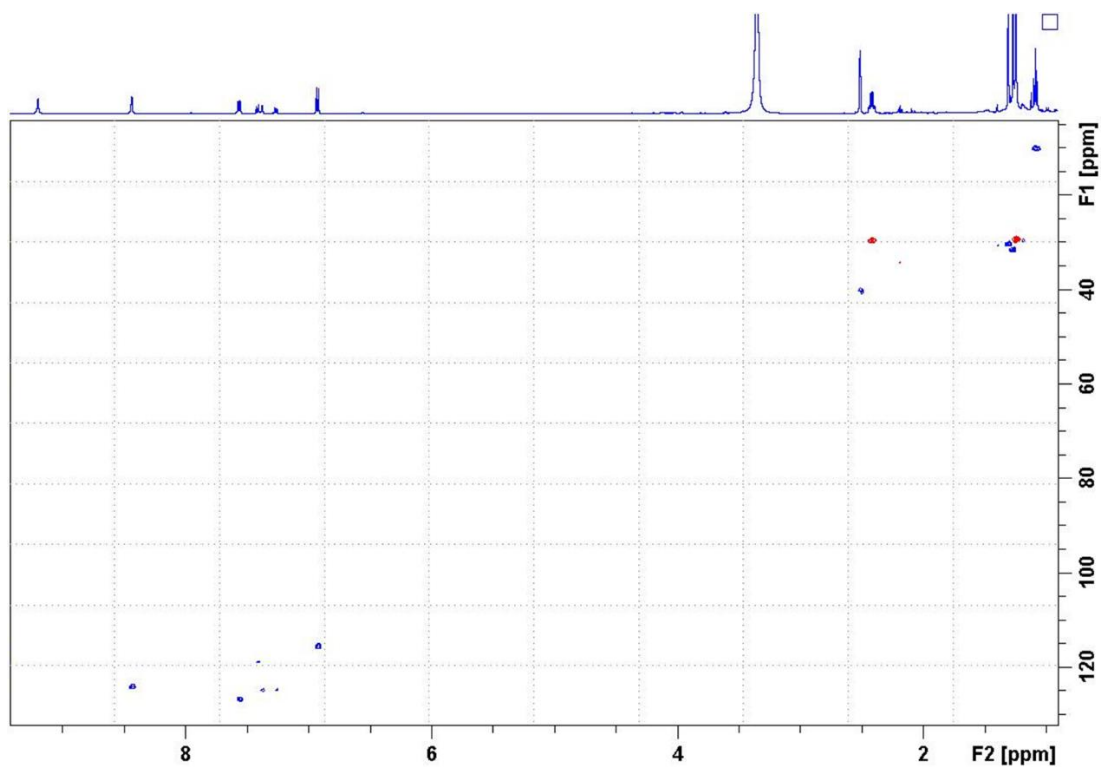


Figure S53. HSQC spectrum of AHB120.

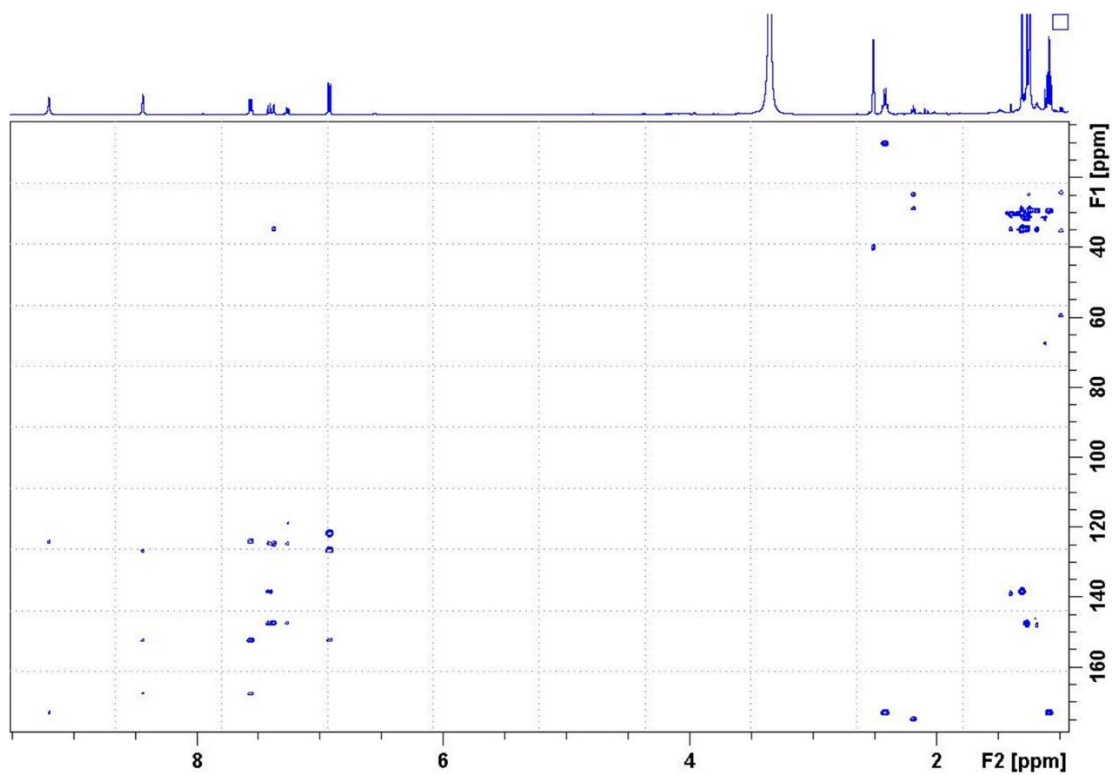


Figure S54. HMBC spectrum of AHB120.